

# The effect of light diffuseness on the outdoor performance of thin film solar cells

Toon Maassen

A thesis presented for the degree of  
Bachelor of Science

Under the guidance of Bruno Ehrler (AMOLF)  
and Wim Sinke (ECN)

AMOLF



UNIVERSITEIT VAN AMSTERDAM



University of Amsterdam

The Netherlands

July 2017

## *Abstract*

Thin film solar cells are claimed to have a higher performance ratio under some light conditions, such as diffuse or low light. In order to investigate whether diffuseness could be a cause for a higher performance ratio of thin film solar cells, we measure the performance of six types of solar cells, while also measuring the irradiance and diffuseness. To measure diffuseness, we developed a cubic illuminance meter and compared its performance with a conventional sun tracker. The diffuseness metric of the cubic illuminance meter correlated with the sun tracker with an  $R^2$  of 0.57 and a p-value of  $3.25 * 10^{-26}$  for the slope of the correlation. An additional advantage of the cube is that it never erroneously exceeds 100% diffuseness. The diffuseness metrics of the cube also had clear correlations with irradiance and temperature, as expected. When selecting the data for small ranges of temperature and irradiance in order to minimize the chance of a spurious relationship, we find that diffuseness has a negative impact on the flexible CIGS module with a slope of  $-3.98 \pm 0.4$  efficiency percentage per normalized diffuseness. Diffuseness has a positive effect on two of the silicon cells;  $2.72 \pm 0.86$  for the HIT Si cell and  $1.94 \pm 1.35$  for the IBC Si cell. While on the CdTe and CIGSm cell the impact was not significant. This means that for the cells that we measured, diffuseness is unlikely to be a cause for a higher performance ratio.

## *Acknowledgements*

This thesis would not have been possible without the welcoming and professional communities of AMOLF and ECN. I want to specifically thank the following people; Bruno Ehrler, for all his time, wisdom and guidance; Wim Sinke, for connecting me to AMOLF and shining his knowledge on my research project; Elio Monaco, Benjamin Daiber and Moritz Futscher, for all their help with Mathematica; Dion Ursem and Henco Schoemaker for their fantastic and never-ending technical support; Nico Dekker and Koen de Groot, for allowing me to and even helping me place a cube next to their sun tracker; Arnoud Jongeling, for sharing his knowledge on 'mutual information'; Maria Stuut and Magdalena Henke for willing to proofread the final result ; Amanda, Jelle, Max and Thomas, who have helped me a great deal in a short time as practicum students. I also want to thank Esmee Jiskoot, Joey Hodde together with the complete De Ceuvel team for taking over some of my responsibilities, which enabled me to carry out this research.

# Contents

<b>Abstract</b>	<b>i</b>
<b>Acknowledgements</b>	<b>ii</b>
<b>1 Introduction</b>	<b>1</b>
<b>2 Theoretical Background</b>	<b>3</b>
2.1 Solar cell physics . . . . .	3
2.1.1 The basic concept of a solar cell . . . . .	3
2.1.2 Characteristics of sunlight . . . . .	5
2.1.3 Important parameters of a solar cell . . . . .	6
2.1.4 Types of solar cells . . . . .	8
2.2 Possible causes for a higher performance ratio of thin film solar cells . . . . .	9
2.2.1 Examples of claims concerning thin film solar cells . . . . .	9
2.2.2 Temperature and photovoltaic efficiency . . . . .	10
2.2.3 Spectrum and photovoltaic efficiency . . . . .	12
2.2.4 Intensity and photovoltaic efficiency . . . . .	13
2.2.5 How diffuseness could impact efficiency . . . . .	14
2.3 Defining diffuseness . . . . .	16
2.3.1 Mathematically comparing the two metrics . . . . .	17
2.4 Statistical analysis . . . . .	18
<b>3 Research Methods</b>	<b>20</b>
3.1 Measuring the irradiance, module temperature, spectrum and module power	20
3.2 Measuring diffuseness . . . . .	21
3.2.1 Cube design . . . . .	21
3.2.2 Comparing the cube with a sun tracker . . . . .	23
<b>4 Results &amp; Discussion</b>	<b>25</b>
4.1 Comparing the cubic illuminance meter with a sun tracker . . . . .	25
4.2 Correlating diffuseness with temperature, irradiance and APE . . . . .	27
4.3 Performance ratios of all six modules . . . . .	28
4.4 Correlating diffuseness with efficiency . . . . .	29
4.5 Influence of irradiance, temperature and spectrum on efficiency . . . . .	32

---

4.6 Influence of diffuseness on efficiency, holding temperature and irradiance constant . . . . .	36
<b>5 Conclusions</b>	<b>39</b>
<b>A 3D drawings of both cubes</b>	<b>42</b>
<b>B Additional graphs; efficiency against diffuseness binned separately</b>	<b>44</b>
<b>C Additional graphs; efficiency against temperature</b>	<b>47</b>

# Chapter 1

## Introduction

The development of efficient solar panels plays a major role in the global transition towards sustainable energy, as solar cells offer an affordable, abundant source of energy, with very little pollution. In order to apply solar cells most appropriately, it is important to clearly understand which factors influence the efficiency of different solar cells. Moreover, for the development of new solar cell designs it is important to understand their properties. Many of the thin film solar cell types are claimed to have a higher performance ratio than silicon cells, i.e. they are claimed to have less of an efficiency drop during some outdoor conditions. In the scientific literature, scientific journalism and in suppliers' descriptions different terms are used to describe the circumstance in which this higher performance ratio occurs. Some examples are 'diffuse light' O'regan and Grfitzeli (1991), but also 'low light' (Heliatek, 2017). The exact factors causing this higher performance ratio are therefore still unclear. This research aims to separate the influence of diffuseness from other factors such as the difference in spectrum, module temperature and irradiance. An extra reason for the relevance of the influence of light diffuseness on the efficiency of solar cells is the development of bifacial solar panels, which always have at least one face in almost completely diffuse light (Janssen et al., 2015).

The research is executed by measuring the efficiency and temperature of six types of commercially available solar cells, while also measuring the irradiance, spectrum and diffuseness of the incoming light. In order to measure diffuseness, a special cubic illuminance meter has been developed, which measures the intensity of the incoming light in six different directions. It therefore is able to quantify to which extent the light comes from all directions or one direction, as a metric for diffuseness. In order to verify the validity of the cube, a second cube is placed next to a more conventional solar tracker, after which the data are compared. The performance data from the solar cells, together

---

with data of the incoming light and the cube, are analyzed to infer what the effect is of diffuseness on the outdoor performance of thin solar cells, when compensating for the effect of other factors. More specifically the goal is to infer whether diffuseness could be a cause for a higher performance ratio of thin film solar cells compared to silicon cells.

## Chapter 2

# Theoretical Background

In the following chapter the necessary theoretical background is laid out. First, a short introduction into solar cell physics is given, explaining the basic concept of a solar panel, the characteristics of sunlight and important parameters of a solar panel. Subsequently, for the four quantities spectrum, intensity, temperature and diffuseness, it is explained with which mechanism it could impact efficiency, and might therefore be a cause for a higher performance ratio of thin film solar cells. Thereafter, an analysis is given of the metric of choice for diffuseness. Finally, the statistical approach to analyzing the data is explained.

### 2.1 Solar cell physics

#### 2.1.1 The basic concept of a solar cell

Solar cells make use of the photovoltaic effect in order to create electric power. The basic component of a solar cell is a semiconductor. A semiconductor is characterized by a separation between the valence band and conduction band as opposed to metals, and a gap smaller than 3 electron-volts (eV) as opposed to insulators (see Figure 2.1).

When a photon with a higher energy than the band gap hits an electron in the semiconductor material, this electron is excited and reaches the conduction band. The electron, therefore, leaves the bonding orbital in an atom and becomes mobile. The excited electron leaves behind the absence of an electron, also called an electron hole. This electron hole effectively behaves as a second mobile charge. After having excited this electron, the goal of a solar cell is to ensure that the electron and hole are separated and transported to a positive and negative electrode, after which the charge can flow through a load, where the added energy of the charges is used. This separation is provided by a  $p$ - $n$

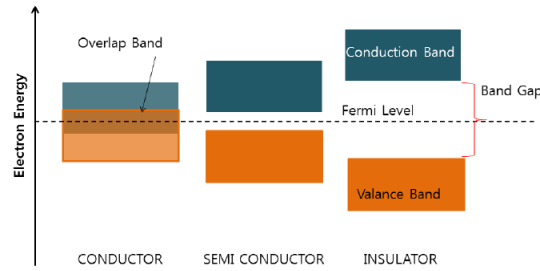


FIGURE 2.1: A schematic band gap diagram of a conductor, semiconductor and an insulator (Mahato et al., 2015)

junction. A  $p$ - $n$  junction is a transition from a  $p$ -doped material to an  $n$ -doped material.  $P$ - and  $n$ -doping are the addition of certain atoms into the lattice of a semiconductor. By choosing an atom which has exactly one bonding electron less or more than the bulk semiconductor, a mobile charge is created, in addition to a fixed charge on the atom itself. When the mobile charge is an electron, it is  $n$ -doped (for negative) and when the created mobile charge is an electron hole, it is  $p$ -doped (for positive). At an interface between  $p$ - and  $n$ -doped materials, some of the mobile charges from the one material will flow to the other and vice versa, due to diffusion. This will create a net charge due to the left behind fixed charges. These in their turn create an electric field, which causes the excited electrons and electron holes to drift in opposite directions, which is the main mechanism with which electrons and electron holes are separated by a  $p$ - $n$  junction (Smets et al., 2016). The effect is schematically shown in Figure 2.2.

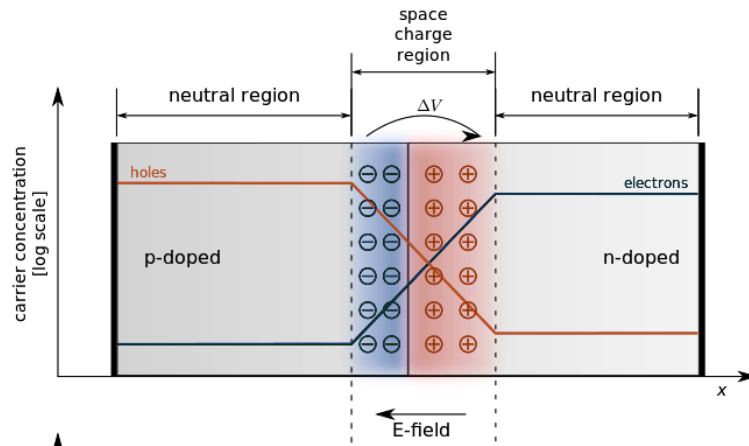


FIGURE 2.2: A schematic diagram of  $p$ - $n$  junction (Christian, 2013)

When an electron and electron hole recombine, the energy of the excited electron is lost. Three main types of recombination can be distinguished; radiative recombination, Auger recombination and Shockley-Read-Hall recombination (SRH). Radiative recombination occurs when the energy of the recombined electron-hole pair is lost to a photon. Auger recombination occurs when the energy of the recombination is transferred to another

electron in the conduction band. This electron reaches an even higher energy, but quickly relaxes back to the lowest available state in the conduction band and the added energy is lost as heat. Shockley Read Hall recombination is assisted by a defect which traps one of the charges in a fixed position (Smets et al., 2016).

### 2.1.2 Characteristics of sunlight

Understanding the characteristics of sunlight on earth is important, as solar panels are meant to absorb sunlight. The sun approximately radiates as a black body radiator. However, when the light passes through the atmosphere, parts of the spectrum are absorbed. As the path length through the atmosphere can vary depending on position on earth and time of the day, the *AirMass* factor ( $AM$ ) is used to quantify this path length. Hereby  $AM$  is the ratio between the actual path length and the path length if the sun were exactly overhead. Figure 2.3 shows the spectrum of the extra terrestrial solar spectrum, of a corresponding black body radiator and of the terrestrial spectrum with  $AM = 1.5$ .

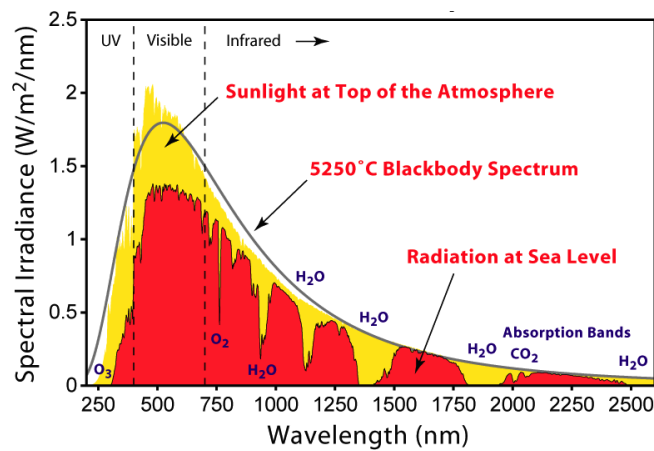


FIGURE 2.3: Extra-terrestrial spectrum,  $AM_0$  (yellow area), black body spectrum (grey line) and terrestrial solar spectrum,  $AM_{1.5}$  (red area). The atmospheric compound responsible for the absorption bands are depicted in blue (Rohde, 2007)

In order to be able to compare the efficiencies of different types of solar cells, standard testing conditions (STC) have been formulated. During an efficiency test, the solar cells are tested underneath a lamp with a solar spectrum of  $AM 1.5$ , at perpendicular incidence, with an intensity of  $1000 \text{ W/m}^2$  and the temperature of the cell is kept constant at  $25 \text{ }^\circ\text{C}$ .

### 2.1.3 Important parameters of a solar cell

Some of the most important parameters that are used to quantify the characteristics of a certain solar cell are the short circuit current density ( $J_{SC}$ ), the open circuit voltage ( $V_{OC}$ ), the fill factor ( $FF$ ), the maximum power ( $P_{max}$ ), efficiency ( $\eta$ ), external quantum efficiency (EQE) and performance ratio (PR). The above concepts are briefly explained below.

$V_{OC}$  is the voltage that a solar cell creates when its electrodes are not connected, in other words when the solar cell is in an open circuit. It is a quantity important to understand what maximum voltage can be created and which fraction of the band gap is really transformed into a voltage.

$J_{SC}$  is the current per area of solar panel that is achieved when the solar cell is connected to a closed circuit. In this case, the excited charges will flow through the closed circuit and no energy is created as there is no voltage over the circuit.

The  $JV$ -curve is a graph that depicts the current density as a function of the voltage. An example of a  $JV$ -curve is shown in Figure 2.4. From this curve, one can infer the maximum power and the fill factor. The maximum power is the power that can be achieved when operating at an ideal combination of voltage and current. This combination is the maximum power point ( $MPP$ ), with corresponding maximum power point voltage ( $V_{mpp}$ ) and current density ( $J_{mpp}$ ). The ratio between  $P_{max}$  and the product of  $J_{sc}$  and  $V_{oc}$  is called the fill factor ( $FF$ ). In Figure 2.4, it represents the ratio between the area of the purple and gray square.

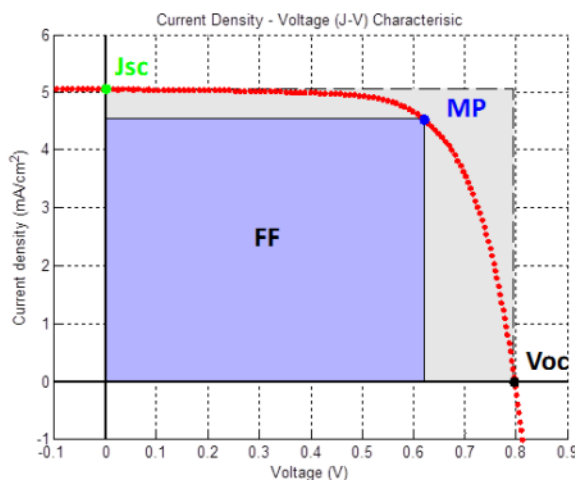


FIGURE 2.4: An example of a measured  $JV$ -curve (Wei, 2015)

Efficiency is the percentage of total incoming power that has been transformed into usable electric power. If one knows the power of the total incoming light, i.e. the

irradiance or light intensity, one can use the  $FF$ ,  $V_{oc}$  and  $J_{sc}$  to calculate the efficiency, see equation 2.1.

$$\eta = \frac{P_{max}}{I_{in}} = \frac{FF \cdot V_{oc} \cdot J_{sc}}{I_{in}} \quad (2.1)$$

As an approximation for the current-voltage relation for most solar cells, the assumption can be made that the current is equal to the short-circuit current minus the leakage current. This leakage current or dark current is the current that flows through a solar cell in the dark when an external voltage or bias is applied. This approximation is called the superposition approximation. It is assumed that the current leaking on the opposite direction in a solar cell in the light, due to the built up voltage over a load by the solar cell itself, is equal to the current that flows through a solar cell in the dark with an external voltage. For an ideal diode, the dark current is equal to (Nelson, 2003):

$$J_{dark}(V) = J_0(e^{qV/k_B T} - 1) \quad (2.2)$$

therefore, the current of a solar cell can be described as:

$$J = J_{sc} - J_0(e^{qV/k_B T} - 1) \quad (2.3)$$

where  $J_0$  is a constant,  $k_B$  is Boltzmann's constant and  $T$  is the temperature in Kelvin. When taking into account both that a real solar cell is a non-ideal diode (with an ideality factor  $m$ ), as well as that there is resistance within the system, which can be divided into a series resistant ( $R_s$ ) and a parallel resistant ( $R_{sh}$ ), the diode equation becomes the following:

$$J = J_{sc} - J_0(e^{q(V+JAR_s)/mk_B T} - 1) - \frac{V + JAR_s}{R_{sh}} \quad (2.4)$$

Whereby  $A$  is the area of the solar panel.

External quantum efficiency ( $EQE$ ) is the percentage of photons of a certain wave length incident on the solar cell that are successfully transformed into an electron-hole pair that reaches the electrodes to contribute to the produced current. It is a measure of how well the material is able to absorb photons of a certain wavelength and is therefore defined in the following way (Smets et al., 2016):

$$EQE(\lambda) = \frac{I_{ph}}{q \cdot \Psi_{ph,\lambda}} \quad (2.5)$$

Where  $\lambda$  is the photon wavelength,  $I_{ph}$  is the photoinduced current,  $q$  is the elementary charge and  $\Psi$  is the photon flux on the panel.

Performance ratio (PR) is the ratio between the achieved efficiency of a solar panel in real sunlight over a long period (such as a year) and the efficiency under standard test conditions. When working with an actual photovoltaic array it can be calculated from the yearly energy produced ( $E_{year}$ ), the total yearly irradiation ( $I_{year}$ ), array area ( $A$ ) and efficiency under STC in the following way:

$$PR = \frac{\eta_{measured}}{\eta_{stc}} = \frac{E_{year}}{I_{year} \cdot A \cdot \eta_{stc}} \quad (2.6)$$

PR is a measure of how well a solar system is performing and how much energy is lost due to the differences between real conditions and STC conditions, such as a varying intensity, temperature, diffuseness, but also inverter inefficiencies, dirt, reflection and downtime (Marion et al., 2005). It is an important quantity for calculating the expected return on investment for a solar system. A similar quantity, however with different units, is the specific energy yield, which is the ratio between the energy produced over a longer period (e.g. a year) in kWh, and the nominal power in Wp (the power a solar cell produces under STC).

#### 2.1.4 Types of solar cells

The large landscape of solar cell types can be categorized using a variety of characteristics, such as the semiconductor material used, the extent of crystallization (such as monocrystalline, multicrystalline and amorphous), the thickness (such as thin film solar cells) or the amount of junctions used (single-junction and multi-junction). Here follows a brief explanation of these different types.

There is a large number of possible semiconductors that can be used as solar cells. The most common, and best researched material is silicon. Commercially available crystalline silicon (c-Si) solar cells have a typical efficiency of 15 to 20 percent and the current record efficiency is 26.7% (Green et al., 2017). Advantages of silicon are the element's widespread availability, its relatively high efficiency and its high stability. A disadvantage is its relatively low absorption coefficient, which necessitates thick panels (Nelson, 2003).

Many of the other materials that can be used as a solar cell are thin film materials. These are characterized as materials with a high absorption coefficient, which makes it possible to use rather thin films as opposed to c-Si. Examples of thin-film materials are copper

indium gallium selenide (CIGS), cadmium telluride (CdTe) and amorphous silicon (a-Si). Advantages of these materials are that they are relatively cheap to produce, light and flexible. This makes it possible to combine these solar panels with building materials such as roofing tiles or walls, and also makes installation easier. Due to their low efficiency though, they have not yet become as competitive as c-Si. Another advantage which this research focuses on is that they are claimed to perform better under some outdoor circumstances such as low intensities, higher temperatures or diffuse light. An important disadvantage is the fact that they commonly use rare earth metals (Smets et al., 2016). Other thin-film materials are still in the phase of research, such as polymer, perovskite, organic and dye-sensitized solar cells. The material that currently holds the highest single-junction efficiency is gallium arsenide (GaAs), with a record efficiency of 28.8% (Green et al., 2017).

Multiple materials can also be combined to create multi-junction or tandem solar cells. In this way, multiple band gaps can be combined to maximize the energy absorption from the incoming photons. The current record efficiency of 38.8% is held by a 5-junction solar cell of GaInAs/GaInP/GaAs/AlGaInAs/AlGaInP (Polman et al., 2016).

## 2.2 Possible causes for a higher performance ratio of thin film solar cells

This section first shows some examples of claims being made concerning thin film solar cells. Thereafter the mechanisms are explained with which temperature, irradiance, spectrum and diffuseness could lead to a higher performance ratio of thin film solar cells.

### 2.2.1 Examples of claims concerning thin film solar cells

Here follow some key examples of different quotes on thin film solar cells, which serve to demonstrate the wide variety of circumstances which are claimed to lead to a higher PR of thin film solar cells. A classical example concerning diffuse light can be found in Nature where O’regan and Grifitzi (1991) stated concerning a dye-sensitized colloidal TiO<sub>2</sub> solar cell;

*“The overall light-to-electric energy conversion yield is 7.1-7.9% in simulated solar light and 12% in diffuse daylight.”*

The supplier of Heliacell, a flexible organic solar cell, makes the following claim on its website (Heliacell, 2017):

*“Superior low light performance. Perfect for façades – even at non-optimal orientation. Up to 25%\* more energy output at low light levels.*

*\* compared to crystalline technology under comparable conditions”*

Similar statements are being made concerning CIGS solar cells, such as the following quote from CIGS White Paper Initiative, pointing at the effect of temperature, spectrum and low intensity in one sentence (White Paper Initiative, 2015);

*“A low temperature coefficient, a favorable spectral response and high efficiency under low light conditions are the reason for excellent energy yields and hence low levelized costs of electricity under most climatic conditions.”*

Concerning the flexible CIGS module that is included in our investigated solar field, the supplier claims the following (Global Solar, 2017):

*“Shade Resistant. Outperforms c-Si modules in partially shady conditions”.*

In short, many different circumstances are claimed to lead to a higher PR of thin film solar cells. In the following subsections the mechanisms are explained behind the main possible causes; temperature, spectrum, irradiance and diffuseness.

### 2.2.2 Temperature and photovoltaic efficiency

Temperature has an effect on the characteristics of a solar panel in multiple ways. For an ideal diode, three main effects can be identified. The increased temperature causes an exponential increase in charge carrier density, which increases the leakage current and therefore decreases the voltage. The increased temperature also causes the valence electrons to reach a higher energy, which leads to a lower band gap energy. This causes on the one hand a higher amount of electrons to be excited, as lower energy photons can now be absorbed. On the other hand, a smaller band gap also leads to a lower  $V_{oc}$ , which decreases the total energy output. There is an increase in photocurrent and a decrease in voltage, which together lead to a net decrease in efficiency (Nelson, 2003). The effect is visualized in Figure 2.5.

Though the above-described effect is the dominant mechanism behind the influence of temperature, other mechanisms can also be identified, such as an increase in recombination due to the increased charge carrier density at higher temperatures. The change

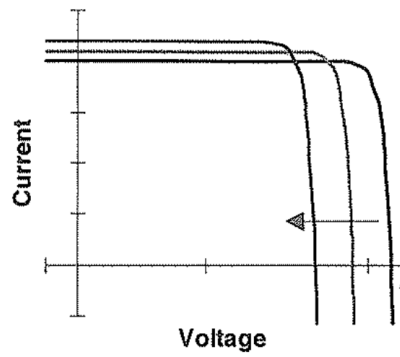


FIGURE 2.5: A visualization of the effect of temperature on a solar cell. The arrow follows subsequent JV-curves with increasing temperature. On the top the current is slightly increasing and at the right the voltage is significantly decreased, which leads to a net decrease of area under the curve and therefore a loss of efficiency. (Nelson, 2003)

in efficiency due to temperatures can vary greatly by material, because the impact on voltage can vary, as well as different types of recombination can be dominant.

The theoretical mechanisms involved in the temperature dependence of thin-film solar cells are less well studied. However, experiments have shown that for a CIGS module the efficiency also decreases with higher temperature (Fathi et al., 2015). Table 2.1 shows which percentage of the maximum power decreases per degree Celsius increase (i.e. the temperature coefficients), for all six investigated panels. It shows that the flexible CIGS module has a remarkably low temperature coefficient, which could lead to a higher performance ratio.

Solar panel	Temp. coefficient
CIGS	0.2136 %/°C
CdTe	0.30 %/°C
Multi Si	not stated
IBC Si	0.43 %/°C
HIT Si	0.29 %/°C
CIGSm	0.30 %/°C

TABLE 2.1: Stated temperature coefficient of the six investigated modules

### 2.2.3 Spectrum and photovoltaic efficiency

Another factor that has to be taken into account is the spectrum of the incoming light, as photons with energy lower than the band gap are absorbed (quantum efficiency) and the extra energy of photons above the band gap energy are lost as heat (quantum defect). In Figure 2.6 the spectral response from a variety of solar cell types is shown. In Figure 2.7 the spectral response of a various CI(G)S modules is shown. It shows that some of CIGS cells have a slightly broader spectral response than silicon cells. It becomes apparent not only that the spectral response can vary greatly between various technologies, but that even within a single technology there can be great variation. This is especially the case for CI(G)S modules (Schweiger et al., 2012).

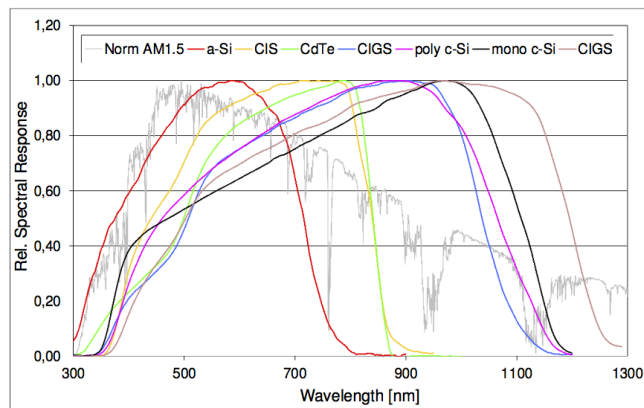


FIGURE 2.6: Spectral response of a variety of solar cell technologies (Schweiger et al., 2012)

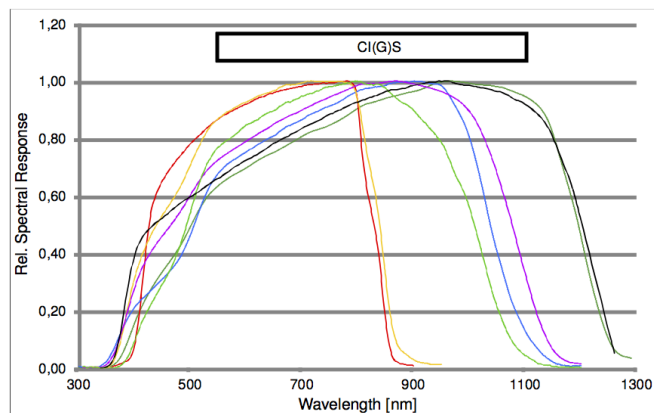


FIGURE 2.7: Spectral response of a variety of CI(G)S modules (Schweiger et al., 2012)

The spectrum of diffuse sunlight commonly differs from the spectrum of direct sunlight. But the type of diffuse light greatly determines the shift of the spectrum. Figure 2.8 shows that the diffuse part of the sunlight during a sunny day is bluer than the normal sunlight spectrum, which is presumably caused by the blue color of the sky. However,

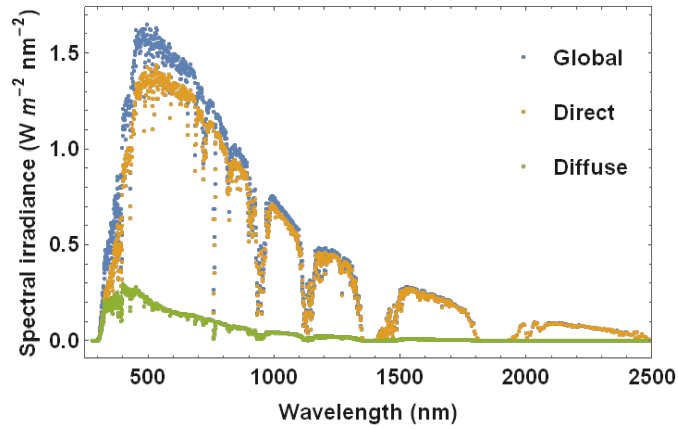


FIGURE 2.8: Spectra of, global, direct and diffuse parts of the sunlight, during a sunny day (Futscher and Ehrler, 2016)

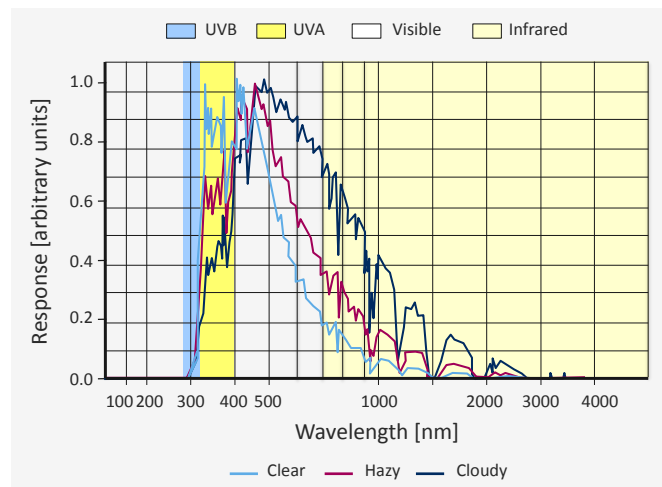


FIGURE 2.9: Spectral shift under weather conditions (Kipp & Zonen, 2012)

the diffuse light during a cloudy day is commonly redder than the normal solar spectrum, as is shown in Figure 2.9. Because some thin film cells have a broader spectral response especially at the red side of the solar spectrum, spectrum could be a factor causing a higher performance ratio for some thin film cells.

The fact that diffuse light can have spectral shifts in both directions also shows that it is important to not use the term ‘diffuse light’ too broadly. It should only be used for the extent to which light comes from all instead of one direction, rather than a light condition concerning more than just its directional characteristics.

#### 2.2.4 Intensity and photovoltaic efficiency

A third quantity that has to be taken into account as a separate factor is intensity or irradiance.

For linear photogeneration and linear recombination the photocurrent will increase linearly with the intensity, as there will be more photons to excite charges (Nelson, 2003, ch. 6). In order to understand what is the influence on the efficiency, one needs to rewrite equation 2.3 in the following way;

$$V_{oc} = \frac{mk_B T}{q} \ln\left(\frac{J_{sc}}{J_0} + 1\right) \quad (2.7)$$

Equation 2.7 shows that the voltage increases with increasing current. This means that the overall efficiency increases with intensity according to the diode equation.

An increase in intensity causes an increase in charge carrier density, which increases the likelihood of electron-hole pairs to find each other to recombine. If this increase is linear, as is the case for SRH recombination, whereby only one of the two recombined charges is mobile, recombination does not impact efficiency during an increased intensity. For Auger and radiative recombination, whereby multiple charge carriers are mobile, recombination will increase quadratically or more with intensity (Smets et al., 2016).

For most silicon panels, SRH recombination is dominant, due to its indirect band gap structure. For other materials with direct band gap structures, nonlinear recombination types are dominant. This could be one of the reasons why most thin film solar cells produce a lower efficiency at higher intensities. Low intensity in this way could be a cause for a comparatively high efficiency of thin film solar cells during outdoor conditions.

### 2.2.5 How diffuseness could impact efficiency

One could think of multiple ways how diffuseness could impact the efficiency of a solar panel. In this section three different mechanisms are explained with which diffuseness could impact efficiency. In diffuse light, light comes from all angles. Diffuseness, therefore, has an impact on the average angle of incidence. This has two effects. First, a larger angle leads to a longer path length through the material. As photons travel through a longer path, a higher percentage of photons is absorbed, which clearly leads to a higher efficiency. However, most solar panels are designed in such a way that almost all of the absorbable photons are in fact absorbed. Hence, this effect is presumably not very large. A second effect of the larger angles is an increase in reflection. As the Fresnel equations dictate, the larger the angle of the incident light beam the larger the reflected part. This leads to a lower efficiency. Figure 2.10 visualizes both effects. Depending on the position of the sun, diffuseness could cause these effects in both directions: when the sun is high an increase in diffuseness means on average larger angles, and when the sun is low an increase in diffuseness means on average smaller angles.

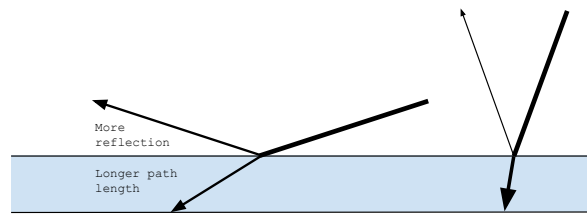


FIGURE 2.10: Reflection and path length under small and larger angles

A third mechanism with which diffuseness impacts the efficiency of a solar panel is through entropy. A solar cell in direct sunlight receives light only from the direction of the sun, while emitting it as a black body radiator in all directions. This increase in angular distribution forms an increase in entropy, and therefore a decrease in efficiency of the solar panel. The magnitude of the effect of an increase in entropy is illustrated by the calculations on a solar cell which limits the directions of emitted light. Researchers calculated that a GaAs single-junction solar cell could theoretically reach an efficiency of 38%, far above the SQ-limit (Kosten et al., 2013).

This loss in entropy does not appear in diffuse sunlight, for both the incident and emitted light are coming from all directions. In this way diffuseness could increase efficiency.

The exact net effect of diffuseness on solar panels is still not clearly studied. A recent study (Mohanty and Wittkopf, 2016) has investigated the effect of diffuseness on a thin film amorphous silicon cell in a lab, by diffusing the light of the test lamp using a fabric. The IV characteristics of the cell were measured, while varying the distance between the fabric and the solar panel (0 and 10 cm, see Figure 2.11). Increasing this distance could be seen as decreasing the diffuseness, for the further away the fabric is from the panel, the more directional characteristics there are. In a preliminary study, they found that the solar panel had a higher current with the fabric at 10 cm than at 0 cm distance (see Figure 2.12). This suggests that this thin film solar cell's efficiency increases with decreasing diffuseness, the opposite of what is commonly claimed.

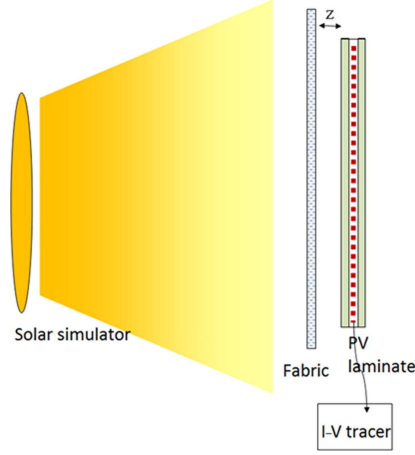


FIGURE 2.11: Setup of diffuseness lab test (Mohanty and Wittkopf, 2016)

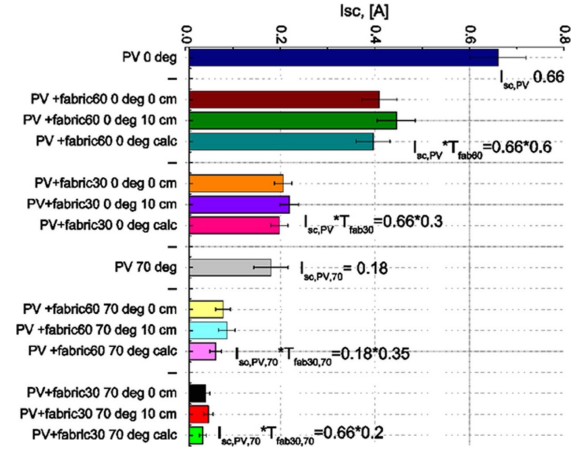


FIGURE 2.12: Results of diffuseness lab test (Mohanty and Wittkopf, 2016)

## 2.3 Defining diffuseness

However common the phrase ‘diffuse light’ may be, the exact definition of diffuseness is definitely not clearly agreed upon yet. There is a wide scale of possible ways to quantify the diffuseness (Xia et al., 2016, 2017). The most common way of measuring diffuseness in the field of solar cell science is using a solar tracker, whereby a light sensor is blocked from direct sunlight and measures all light that comes from directions other than the sun, which is interpreted as the diffuse fraction. In this way diffuseness is the percentage of light coming from other directions than the sun.

For the cubic illuminance meter used in this study, a different metric is used. Hereby the more subtle ‘flow of light’ or ‘ratio between illumination vector and scalar’ by Cuttle (1967) is used. It is able to quantify the diffuseness of the light by measuring the light in six opposite directions. The following calculation is used:

$$\mathbf{E}_{vector} = (E_{+x} - E_{-x}, E_{+y} - E_{-y}, E_{+z} - E_{-z}) \quad (2.8)$$

$$E_{scalar} = \frac{|\mathbf{E}_{vector}|}{4} + \frac{\min(E_{+x}, E_{-x}) + \min(E_{+y}, E_{-y}) + \min(E_{+z}, E_{-z})}{3} \quad (2.9)$$

$$(D_{Cuttle})_{Normalized} = 1 - \frac{|\mathbf{E}_{vector}|/E_{scalar}}{4} \quad (2.10)$$

Whereby  $E_{+x}$ ,  $E_{-x}$ ,  $E_{+y}$ ,  $E_{-y}$ ,  $E_{+z}$  and  $E_{-z}$  are the six measurements of the light sensors on the cube, and ‘min’ is the minimum of two values.  $(D_{Cuttle})_{Normalized}$  is the final diffuseness metric between 0 and 1, whereby 1 is completely diffuse and 0 is completely directional.

Our measurements showed that this metric is more or less equal to the more simple calculation of the sum of the absolute differences between opposite sides divided over the total:

$$(D_{Cuttle})_{Normalized} \approx \frac{|E_{+x} - E_{-x}| + |E_{+y} - E_{-y}| + |E_{+z} - E_{-z}|}{E_{+x} + E_{-x} + E_{+y} + E_{-y} + E_{+z} + E_{-z}} \quad (2.11)$$

This second calculation (eq. 2.11) gives a good qualitative understanding of what the metric represents.

### 2.3.1 Mathematically comparing the two metrics

In order to gain an idea of the differences between the metrics of diffuseness used for the sun tracker and cube, we developed the following mathematical model. In this model daylight is divided into three fractions: direct sunlight, diffuse sunlight, and reflected sunlight. The direct fraction of the sunlight comes exactly from the direction of the sun, the diffuse fraction of the light is all the light coming from the sky but not from the sun, and is assumed to decrease as its direction is further from the sun. Then there is also the reflected light, which is all the light that is reflected from earth's surface. These three fractions could be described in the following way:

$$\begin{aligned} f_{dir}(\theta) &= 1 \quad \text{if } \theta < \frac{1}{2}^\circ \\ &= 0 \quad \text{otherwise} \end{aligned} \quad (2.12)$$

Whereby  $\theta = 0, \phi = 0$  is the position of the sun, and  $\frac{1}{2}^\circ$  is the angle of the sun on the sky.

$$f_{dif}(\theta) = \frac{1}{\theta^b} \quad (2.13)$$

This creates a diffuse light function from all over the sky, but the light increases as it comes closer to the direction of the sun.  $b$  is a constant which determines the extent to which the diffuse light is coming from all over the sky (very cloudy), or mainly from around the sun (less cloudy).

$$f_{ref}(\theta) = \frac{1}{(\pi - \theta)} \quad (2.14)$$

The above equation is similar to  $f_{dif}(\theta)$ , however now it comes from the opposite direction, from below, as it represents the reflected light. In Figure 2.13 a plot is shown of these functions.



FIGURE 2.13: Plot of direct, diffuse and reflected part of the modeled light function

Now the total light is a combination of these three parts:

$$\begin{aligned}\Phi &= c_{dir} \cdot f_{dir}(\theta) + c_{dif} \cdot f_{dif}(\theta) + c_{ref} \cdot f_{ref}(\theta) \\ &= c_{dir} \cdot f_{dir}(\theta) + c_{dif} \cdot \frac{1}{\theta^b} + c_{ref} \cdot \frac{1}{(\pi - \theta)^b}\end{aligned}\quad (2.15)$$

A solar tracker measures the value of the diffuse light ( $c_{dif}$ ) and the value of the direct light ( $c_{dir}$ ). It would be more precise to say it measures a hemispherical integral over the total light function excluding the sun, compared to a hemispherical integral including the sun. The cubic illumination meter, however, measures the total intensity in six opposite direction. Which could be understood as integrating over six hemispheres of the total light function. What becomes apparent here is that the cube is far more dependent on the reflected light coming from below, than is the solar tracker. This makes the cube especially fit for research on bifacial solar panels. For monofacial solar panels, however, this is a disadvantage. Another difference is that the cube is able to extract more information of the directional characteristics of the diffuse fraction of the light.

In further research, these integrations could be calculated in order to come to a theoretical mathematical relation between the two measures of diffuseness. One can already derive from this model though, that an always valid relation between the two metrics does not exist, for the relation is dependent on the amount of reflection coming from below.

## 2.4 Statistical analysis

As we are measuring solar cells in real light environments as opposed to a lab experiment, statistical tools are necessary to distinguish the effects of different factors. Because many factors are impacting the solar cell performance, a correlation between two variables does

not imply causation, as there may be a spurious relationship. A spurious relationship is an apparent relationship, which is actually caused by a third factor which impacts both other variables. This third factor is called a confounding factor (Burns, 1997). This research is investigating whether diffuseness could be a cause for a higher PR of thin film solar cells. For this we need to compare the effect of diffuseness on the efficiency of thin film solar cells and silicon solar cells. The possible confounding factors that we have selected are module temperature, irradiance and APE.

With the goal of identifying the sole effect of diffuseness we carry out the following procedure. First, we check for correlation between diffuseness and the possible confounding factors. When there is a clear correlation, it means that the factor has to be taken into account as a possible confounding factor. Secondly, we graph the correlation between these other factors and efficiency, in order to better understand the effect of these factors. Finally, we graph the correlation between diffuseness and efficiency, while selecting for small ranges - or 'bins' - of the confounding factors. In this way the impact that the other factors might have is minimized as the data shows only a very small variation of those factors. A disadvantage of this method is the large amount of data that is unused. Hence, it is necessary to work with a high amount of measurements.

If diffuseness has a more positive effect on the performance of thin film solar cells than on silicon cells, it means that diffuseness could be a reason for higher performance ratios of thin film solar cells.

## Chapter 3

# Research Methods

### 3.1 Measuring the irradiance, module temperature, spectrum and module power

At the AMOLF institute there is a setup of six types of commercially available solar panels. Figure 3.1 shows a picture of the solar panels. Table 3.1 shows the six different solar panel types and characteristics.



FIGURE 3.1: A picture of the AMOLF solar field.

Three out of the six solar panels are thin film solar cells; CIGS, CIGS with back mirror and CdTe. The others are specific types of silicon cells; a multicrystalline silicon cell, a highly efficient monocrystalline silicon cell, whereby all contacts are placed at the back

Module #	Name	Dimensions (m x m)	Band gap (eV)	nominal efficiency (%)
1	Copper Indium Gallium Selenide (CIGS)	2.017 x 0.494	1.2	12.7
2	Cadmium Telluride (CdTe)	1.200 x 0.600	1.45	12.0
3	Multicrystalline Silicon (Poly-Si)	1.675 x 1.001	1.12	15.5
4	Integrated Back Contact Monocrystalline Silicon (IBC Si)	1.559 x 1.046	1.12	32.5
5	Heterojunction Intrinsic Layer Monocrystalline Silicon (HIT Si)	1.580 x 0.798	1.12	19.3
6	Copper Indium Gallium Selenide with back mirror (CIGSm)	1.656 x 0.656	1.2	32.5

TABLE 3.1: A table of the characteristics of the 6 analyzed solar panels.

(integrated back contact), and a heterojunction intrinsic layer monocrystalline silicon. Every five minutes a large variety of quantities are measured for these solar cells, such as the  $V_{oc}$ ,  $J_{sc}$ , efficiency, FF and module temperature. In addition, the weather and incoming light characteristics are measured, using a spectrometer, pyranometer and a weather station (De Hart, 2016).

Specifically for this research, a cubic illuminance meter has been added to this solar field, which also measures every five minutes. We have gathered data from this setup for over a month, from 22 May until 26 June 2017. The cube has been placed behind and above the solar panel array, placed exactly in the plane of the panels to minimize reflection of the panels on the cube. The details of this cube are explained in the following section.

## 3.2 Measuring diffuseness

In the need to measure light diffuseness in an easy and affordable manner, a cubic illumination meter has been designed and built. The design was inspired by the work of Cuttle (2014) and Xia et al. (2016, 2017), whereby a similar cube is used in the field of light design and interior architecture. As such a cube is new to the field of solar cell science, we have executed a comparison to verify the validity of this method. In the following chapter the cube design is laid out, as well as the setup for this comparison.

### 3.2.1 Cube design

For this research two cubes have been built, one for measuring the light incident at the solar panels and another for comparing the cube to a more conventional method of quantifying diffuseness, a solar tracker. Both cubes are ten x ten x ten centimeters, are colored black to minimize light reflection and have a light intensity sensor on each face. As sensors we have used the Yoctopuce Light V3 modules, which consist out of a lux sensor (BH1751FVI produced by ROHMS) and a command sub-module which is able to directly communicate the sensor signal to a computer through a USB cable. This model

is able to measure light intensity with an error of 1.4 lux, which is a remarkable precision, given the measurement range of 100.000 lux. The sub-modules with USB connection enable us to integrate the system without having to construct any circuits. The sub-modules are separated from the sensor and reconnected with soldering cables, to be able to place the sensor on the outside of the cube and the sub-modules safely inside. All sub-modules are connected through USB-cables, which leave the cube through a hole at the bottom of the cube.

The first cube is made by laser cutting black plastic into six squares, on each of these squares the sensors are attached and the squares are glued together into a cube. In order to weather proof this cube, another cube is formed around the inner cube made out of six squares of transparent perspex glass. The inner and outer cubes are connected through 3D-printed edges.

The second cube is made from black painted metal, which is cut and bent into three parts, all making two faces of the cube. Instead of building a second cube for weather proofness, watch-glasses are placed over the sensors. Although the design is slightly different the concept is still very much the same.

In appendix A 3D drawings of both cubes are attached.



FIGURE 3.2: A picture of the different parts of the first cube.



FIGURE 3.3: The first cube being placed next to the solar field.



FIGURE 3.4: A picture of the second cube at ECN.

### 3.2.2 Comparing the cube with a sun tracker

In order to gain an idea of how the cube measures diffuseness, we have placed one of the self-made cubes next to a commercially available Solys Sun Tracker at the *Energieonderzoek Centrum Nederland* (ECN). This sun tracker, from the supplier Kipp & Zonen, measures diffuseness by separately measuring the total, diffuse and direct part of the light. This apparatus uses pyranometers as light sensors, which are able to measure all incoming light irrespective of the spectrum, by measuring the heat light creates. A small black hemisphere is constantly following the path of the sun, in order to block the direct sunlight on one of the pyranometers. In this way, the total intensity of the light coming from other directions than the sun is measured, which is interpreted as the total



FIGURE 3.5: A picture of the cube and sun tracker at ECN.

intensity of the diffuse light. A second pyranometer is measuring in all directions (the 'global light').

Four meters from this sun tracker the cubic illuminance meter is placed on top of a 1.6 m long pole. As explained, the cube measures the intensity of the light in six directions. The equations of Cuttle (1967) are applied to these values, in order to quantify to which extent the light comes from all directions or one direction, as a metric for diffuseness.

A picture of the setup is shown in Figure 3.5.

## Chapter 4

# Results & Discussion

In this chapter the results of our research are presented and discussed. First, we present the results of the comparison between the self-made cubic illuminance meter and the commercially available sun tracker. Second, we show how our diffuseness metric correlates with other variables such as temperature, irradiance and APE. Third, we show the correlation between solar cell efficiency and diffuseness. Fourth, we plot the correlation between efficiency and other possible confounding factors. Finally, we show the correlation between diffuseness and solar cell performance, while selecting for possible confounding factors.

### 4.1 Comparing the cubic illuminance meter with a sun tracker

In order to verify the validity of the cubic illuminance meter, we have stationed a second cube next to a sun tracker at ECN. After a week of measuring it became apparent that the second cube is not well protected against rain, for water condensed at the inside of the watch glasses. This means that for the comparison only the first 1.5 day of data is usable, the time before it started raining. Figure 4.1 (a) shows the data of the cube (yellow) and the data of the sun tracker (blue).

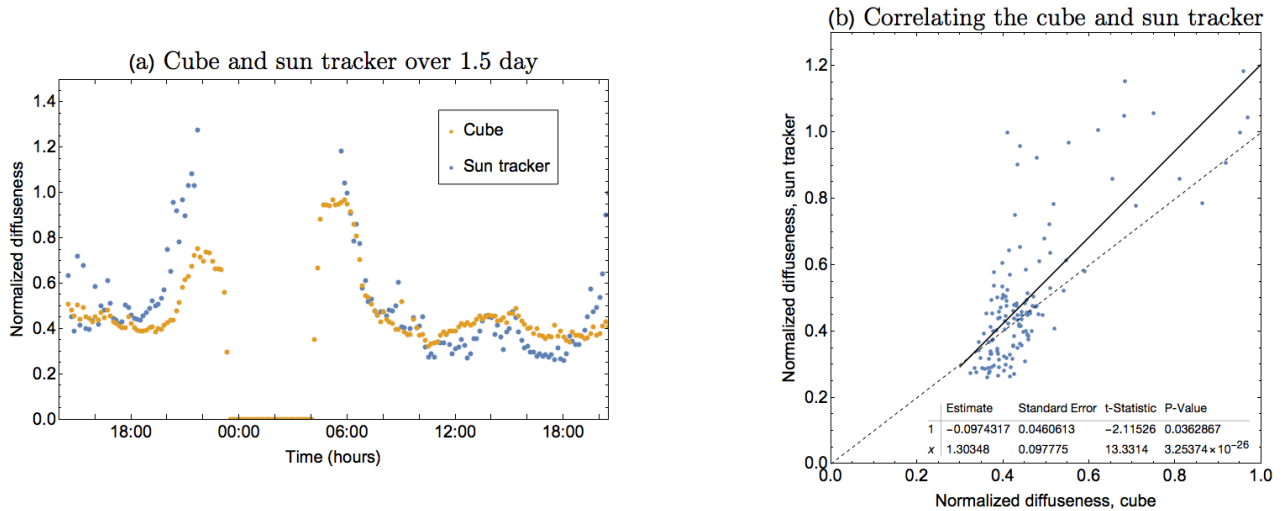


FIGURE 4.1: Diffuseness measured by the sun tracker and cube over time (a) and the correlation between both metrics (b). The dotted line represents the  $x = y$  line and the black line shows a linear fit.

At first sight, the graph definitely shows a correlation between the two metrics of diffuseness. This is quite remarkable, for they are qualitatively a different metric. When examining this graph, a variety of findings can be made. First, in the early morning and late night, the value of the sun tracker can exceed 1, which are non-physical values. It means that at some points in time, the pyranometer for the diffuse light measures a higher value of irradiance than the pyranometer for the global light. This measurement error could be caused by shadow which only falls on the global pyranometer, or artificial light falling on the diffuse pyranometer. For the cube this problem does not arise, as it is mathematically impossible for its metric to exceed 1.

In order to quantify the correlation, both metrics have been graphed against each other in Figure 4.1 (b). The dotted line shows the line of  $x = y$  and the black line shows a linear fit for the data. The statistical parameters have been displayed below the graph. Although there is some scattering especially at higher diffuseness levels, there is a clear correlation, with an  $R^2$  of 0.574 and a p-value of  $3.25 \times 10^{-26}$  for the slope of the fit. The scattering at higher diffuseness values is mainly caused by the slight diverging of the two metrics after around 18:00 (see Figure 4.1 (a)). This is presumably caused by a combination of the following two effects. First, the measurement error of the sun tracker, whereby the diffuseness exceeds 1, might have caused an incorrect increase of measured diffuseness already below 1. This might explain the diversion of the two metrics. Another factor which could play a role is the characteristics of the evening light at the ECN, which is located right at the seaside. The reflection of the sun on the sea could be registered as diffuse light by the sun tracker, as it does not originate exactly

from the direction of the sun. Whereas it is registered as rather direct light by the cube, because it is still coming from mainly one direction.

As expected, these two metrics can not be correlated perfectly as they are different ways of defining diffuseness itself. A longer time of measuring could potentially further clarify the relationship. These first 1.5 of day of measurements, however, show a correlation and highlight a potential for the cubic illuminance meter.

## 4.2 Correlating diffuseness with temperature, irradiance and APE

The other cube, that measured diffuseness next to the solar panels, did survive all rain and weather. This means that we have data for over 33 days of the diffuseness as well as the performance of the solar cells, the incoming radiation and spectrum. In order to infer how diffuseness relates with other possible factors impacting the efficiency, the diffuseness data is compared with module temperature (T), average photon energy (APE) and irradiance (I). Figure 4.2 shows the relation between diffuseness and irradiance (a), module temperature (b) and average photon energy (c). For the module temperature the CIGSm module has been chosen, as a representative module for thin film solar cells. The yellow dots are the median of the data groups, grouped for small steps in the x-variable. The height of the error bars display the median deviation, and the black line is a linear fit of the data. Below the graphs, the residuals of the fit, as well as some statistical parameters, are depicted. The data show that diffuseness consistently decreases with irradiance, the fit has a slope of  $0.123 \pm 0.012$  diffuseness decrease per 1000  $\text{W}/\text{m}^2$ . Diffuseness decreases consistently with module temperature;  $0.0021 \pm 0.00021$  decrease in diffuseness per  $^{\circ}\text{C}$ . There is no clear correlation between diffuseness and APE, with a p-value of the slope of the fit far above 0.05.

The fact that both temperature and intensity correlate with diffuseness indicates that statistical tools will be necessary to separate the effect from diffuseness and the other two variables. Furthermore, it shows that the cubic illuminance meter appears to measure a sensible quantity, as it is expected that diffuseness correlates with temperature and irradiance.

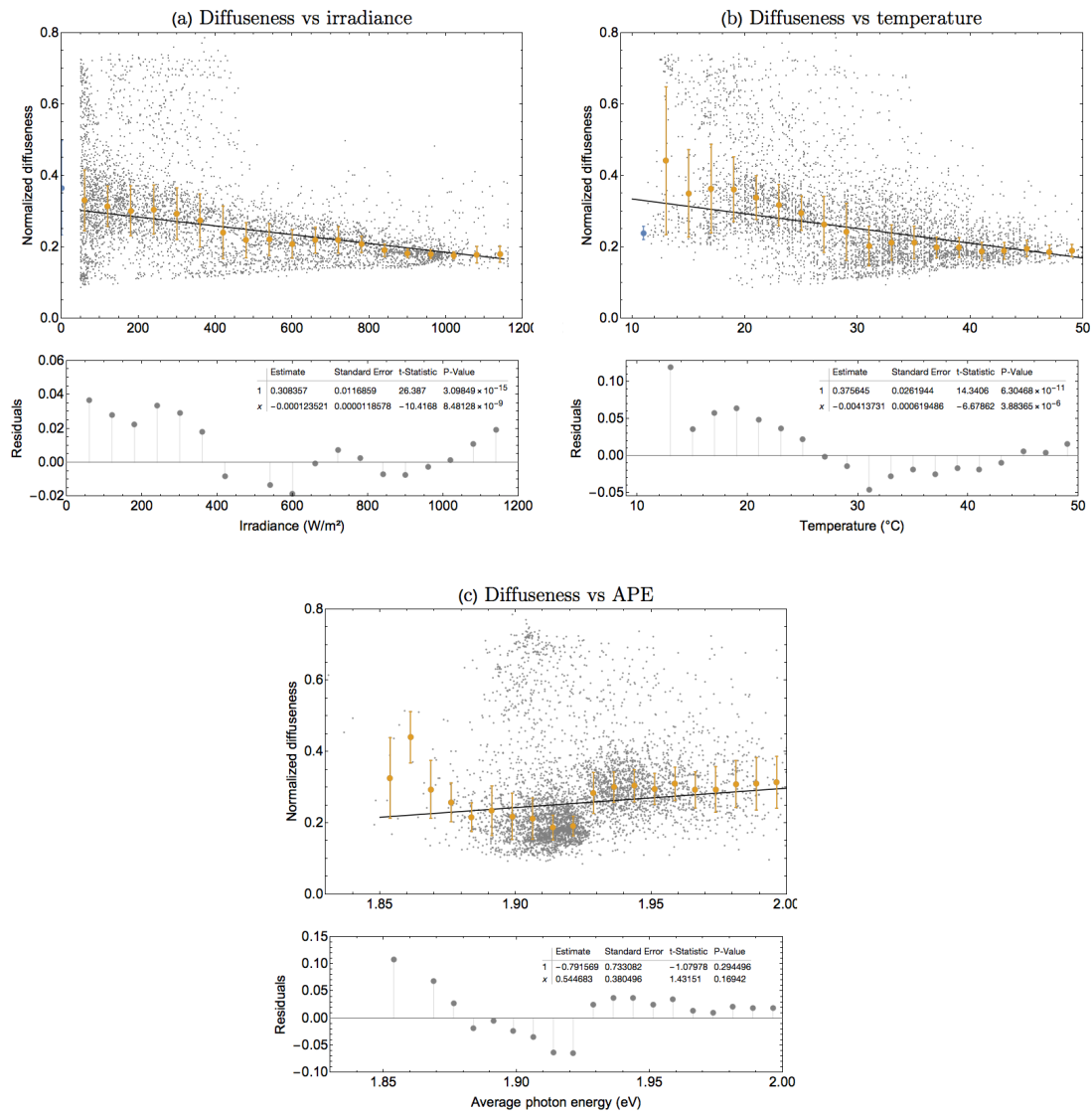


FIGURE 4.2: Diffuseness against module irradiance (a), module temperature (b) and average photon energy (c). Gray dots represent single data points and yellow dots are the average over a small range of the x variable. The error bars show the median deviation. The black line is a linear fit for the data and below the graphs are the residuals as well as statistical parameters.

### 4.3 Performance ratios of all six modules

The motivation for this research is that many thin film solar cells have a higher performance ratio than silicon cells. In order to verify to which extent this premise is valid for the investigated solar panels, we calculate the PR of all the six module types. The PR has been calculated by taking the median efficiency over the total measuring period and dividing this over the stated STC efficiency.

Solar panel	PR over a month	PR over a year
CIGS	63.6%	62.2%
CdTe	68.7%	56.2%
Multi Si	92.4%	93.3%
IBC Si	93.7%	87.7%
HIT Si	93.0%	86.8%
CIGSm	100.98%	95.5%

TABLE 4.1: Performance ratio of all six modules over a month (20 May until 22 June 2017), and a year (July 2016 until May 2017)

Table 4.1 shows the PR values, calculated over the period of a month (the period in which the cube also measured), and a period of a year (before having installed the cube). It shows that the CIGSm module has indeed remarkably high performance ratios, even exceeding the STC efficiency in June/May, and having the highest PR when calculated over a full year (95.5%). The other two thin film types however (CIGS and CdTe) have a remarkably low performance ratio of around 60 percent. This might be caused by the partial shading by the tree or building next to the solar field, leading to unrealistically low efficiencies. It does mean that the panel of most interest to our research is the CIGSm panel, as we are sure it has the higher performance ratios that we are investigating. Despite their low PR, we will continue to include the flexible CIGS and CdTe modules in our results, as it is still relevant to understand how they are impacted by diffuseness.

#### 4.4 Correlating diffuseness with efficiency

Now that we have gained insight in the validity of the cube, the correlations between diffuseness and temperature, irradiance and APE and have gained insight in the the PR of the modules, we move on to correlating the measured factors with the performance of the solar cells. In this section, we show the correlation between diffuseness and solar cell efficiency. Note that in these graphs we have not yet selected for specific ranges of possible confounding factors. This means that these correlations do not imply causation.

In these graphs some interesting trends become apparent. First of all, for the flexible CIGS module the efficiency decreases with diffuseness and for all other modules, efficiency increases with diffuseness. This might be caused by the fact that this is the only

---

flexible panel, and has a polymer rather than glass cover. The question now however is, to which extent this is caused by diffuseness itself or by other circumstances that go together with diffuseness, such as low temperatures and low irradiance. More specifically the question is whether the influence of diffuseness is larger for the CIGSm cell than for the silicon cells, so that it could be a cause for the relatively high performance ratio.

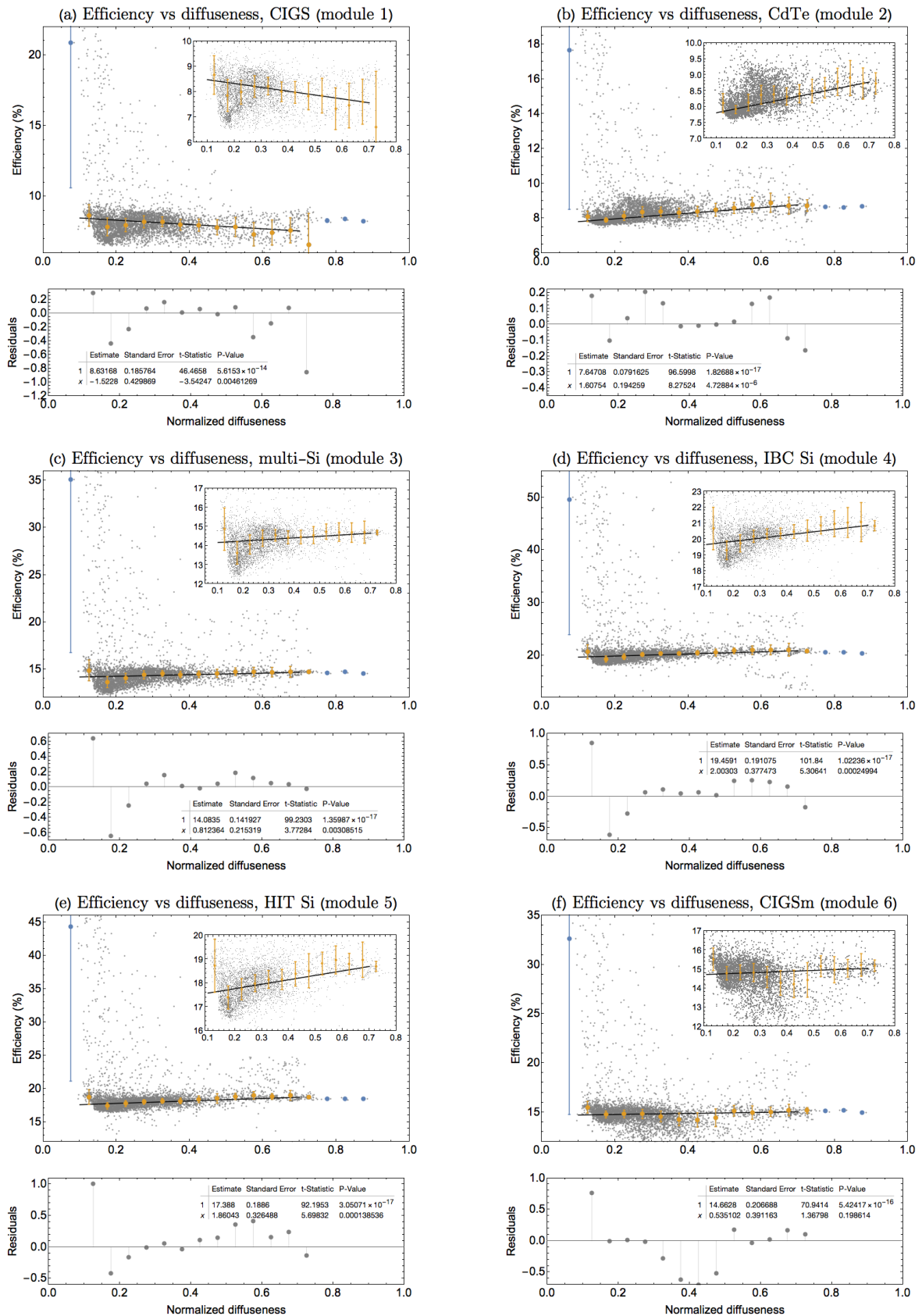


FIGURE 4.3: Efficiency against diffuseness for all six modules. Gray dots represent separate data points, yellow dots represent the median efficiency over a range of 0.05 of diffuseness, blue dots are not used in the fit as they represented too little data or were unrealistic values of efficiency. Error bars show the median deviation. The black line is a linear fit of the data and below the graphs are the residuals as well as the statistical parameters.

## 4.5 Influence of irradiance, temperature and spectrum on efficiency

As a first step in answering the question whether the influence of diffuseness is caused by diffuseness itself or could be caused by other constants, we graph the influence of irradiance, spectrum (average photon energy) and module temperature against efficiency. Figure 4.4 shows the influence of irradiance on efficiency. It becomes clear that from 200 to 1000 W/m<sup>2</sup> efficiency decreases with increasing irradiance for all six types of solar panels. The effect is presumably mainly caused by the increase in module temperature caused by the increase in irradiance. Above 1000 W/m<sup>2</sup> however, all modules, except for CdTe, efficiency increases slightly with irradiance. The fact that efficiency increases for low-irradiance levels shows that it is indeed possible that lower irradiance is causing the increased efficiency of diffuseness.

Figure 4.5 shows the influence of module temperature on efficiency. Here, a very clear relation is visible, whereby as expected an increasing temperature causes a decreasing efficiency. This means that temperature could also be a cause for the positive correlation between efficiency and diffuseness.

Figure 4.7 shows the influence of average photon energy on the average efficiency. Efficiency seems to decrease with average photon energy. An interesting pattern is visible in which the efficiency decreases strongly until 1.9225 eV, then suddenly goes back to higher levels to slowly decrease again. In order to show the cause of this effect, we have colored all data points according to the temperature. This clearly shows that the downward peak has a large amount of points with temperatures between 40 and 50 °. The effect is therefore not caused by APE but by the negative effect on efficiency by temperature. In the region of 1.93-2.0 eV where the temperature appears more or less constant, there still is a downwards trend in efficiency with increasing APE. This suggests that the effect of quantum defect is larger than the effect of EQE. Strikingly the CdTe module has an upwards trend in this region, which suggests that for CdTe the EQE is more dominant than the quantum defect. As diffuseness was not correlating well with APE, APE can not be the cause for the correlation between efficiency and diffuseness. However, it is a separate factor that could be part of the high performance ratio of a thin film solar cell. Figure 4.7 also shows the relevance of small ranges of possible confounding variables, as a pattern between APE and efficiency was actually caused by temperature.

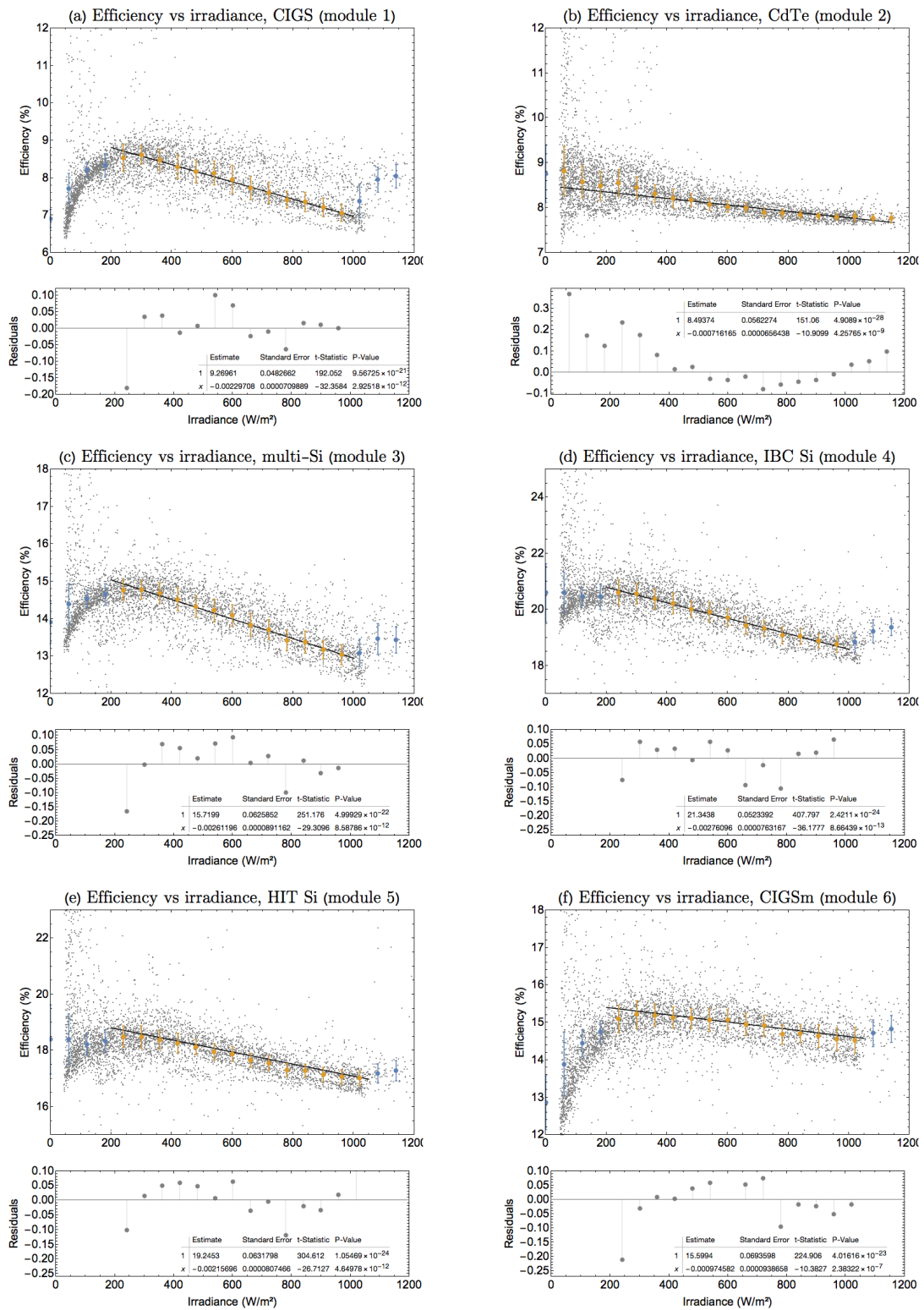


FIGURE 4.4: Efficiency against irradiance for all six modules. Gray dots represent separate data points, yellow dots represent the median efficiency over a small range of temperature, blue dots are not used in the fit in order to fit the slope between 200 and 1000  $W/m^2$ . Error bars show the median deviation. The black line is a linear fit of the data and below the graphs are the residuals as well as the statistical parameters.

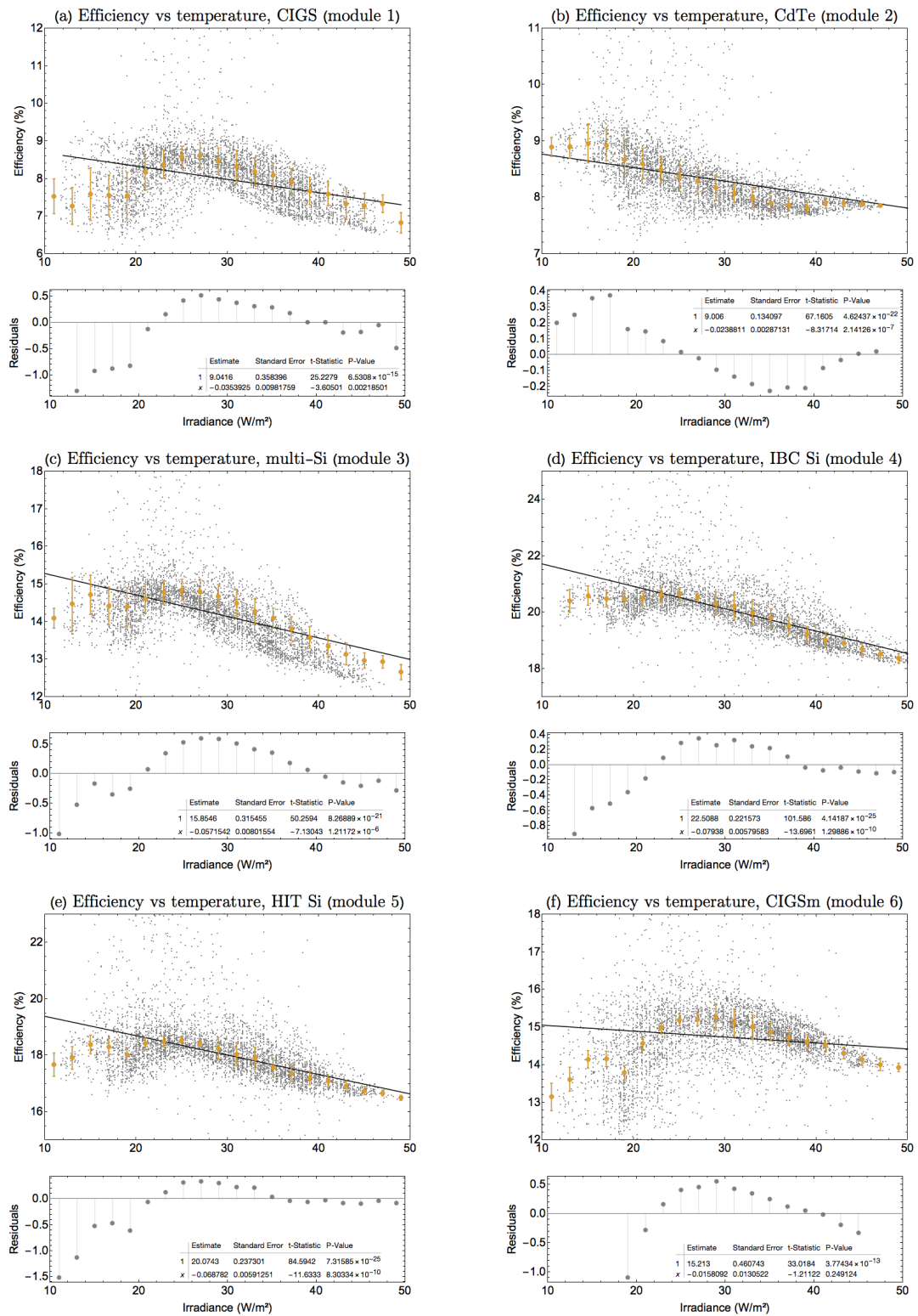


FIGURE 4.5: Efficiency of the six different modules vs module temperature. Gray dots represent separate data points, yellow dots represent the median efficiency over a small range of temperature. The error bars show the median deviation. The black line is a linear fit of the data and below the graphs are the residuals as well as the statistical parameters.

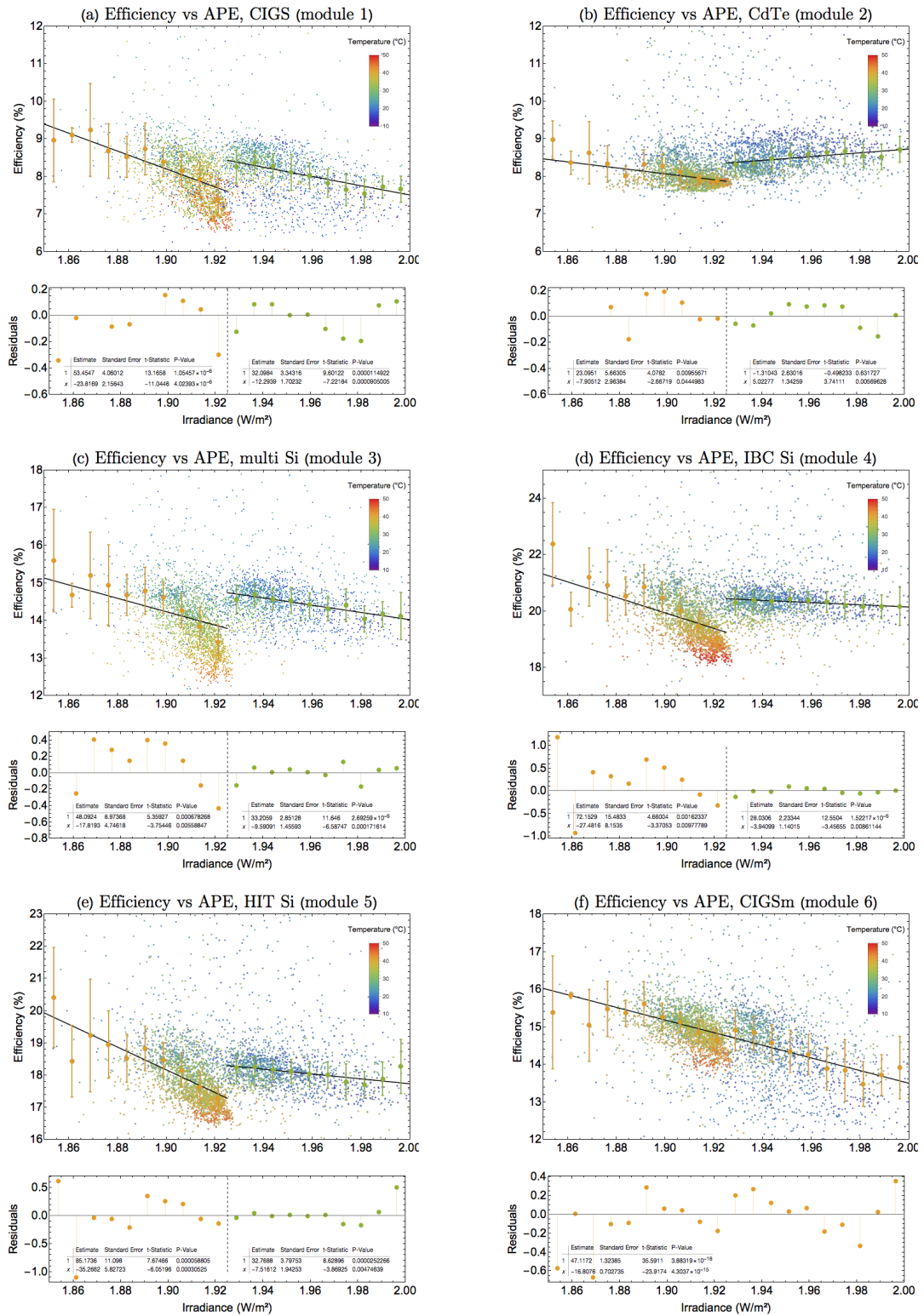


FIGURE 4.6: Efficiency of the 6 different modules against average photon energy. Small dots represent separate data points and are colored according to the module temperature. Yellow and green dots represent the median efficiency over a small range of temperature, whereby the yellow dots have been used for the first fit and the green dots have been used for the second fit. The error bars show the median deviation. The black lines are a linear fit of the data and below the graphs are the residuals as well as the statistical parameters.

## 4.6 Influence of diffuseness on efficiency, holding temperature and irradiance constant

The previous sections have shown the basic correlations between efficiency and diffuseness, as well as the correlation between efficiency and possible confounding factors. Because irradiance and temperature correlate well with diffuseness and have a similar correlation with efficiency, they might be the cause behind the relation between diffuseness and efficiency. In order to deduce whether diffuseness has any influence by and of itself, we plot the efficiency versus diffuseness, while selecting small ranges for other quantities.

Figure 4.7 shows the efficiency versus diffuseness for all six solar panel types. The graph only shows the data points for which irradiance is between 100 and 250 W/m<sup>2</sup> and the temperature is between 20 and 26 °C. In order to qualitatively verify whether the trend is not caused by APE, we have colored the data points according to the APE value.

Now that we have both colored and binned for the three possible confounding factors, the following observations can be made. As an exception to the six modules, the efficiency of the flexible CIGS module is negatively impacted by diffuseness. The fit has a strong negative slope of  $-2.20 \pm 0.49$  efficiency percentage point per normalized diffuseness metric. This exceptional case might be caused by the special characteristics of this flexible module, which has a polymer coating as opposed to a glass cover. It is a remarkable result, as the supplier of this solar cell claimed the cell to be ‘shade resistant’. The CdTe and the CIGSm solar cell appear not to be significantly impacted by diffuseness, as the p values of the slope far exceed 0.05, and the standard error of the slope is almost equal to the slope itself. For the IBC and HIT silicon solar cells however, diffuseness significantly impacts efficiency, whereby the slope of the fit is  $1.36 \pm 0.35$  for the HIT Si cell and  $2.42 \pm 0.29$  for the IBC Si cell (in efficiency percentage points, per normalized diffuseness metric).

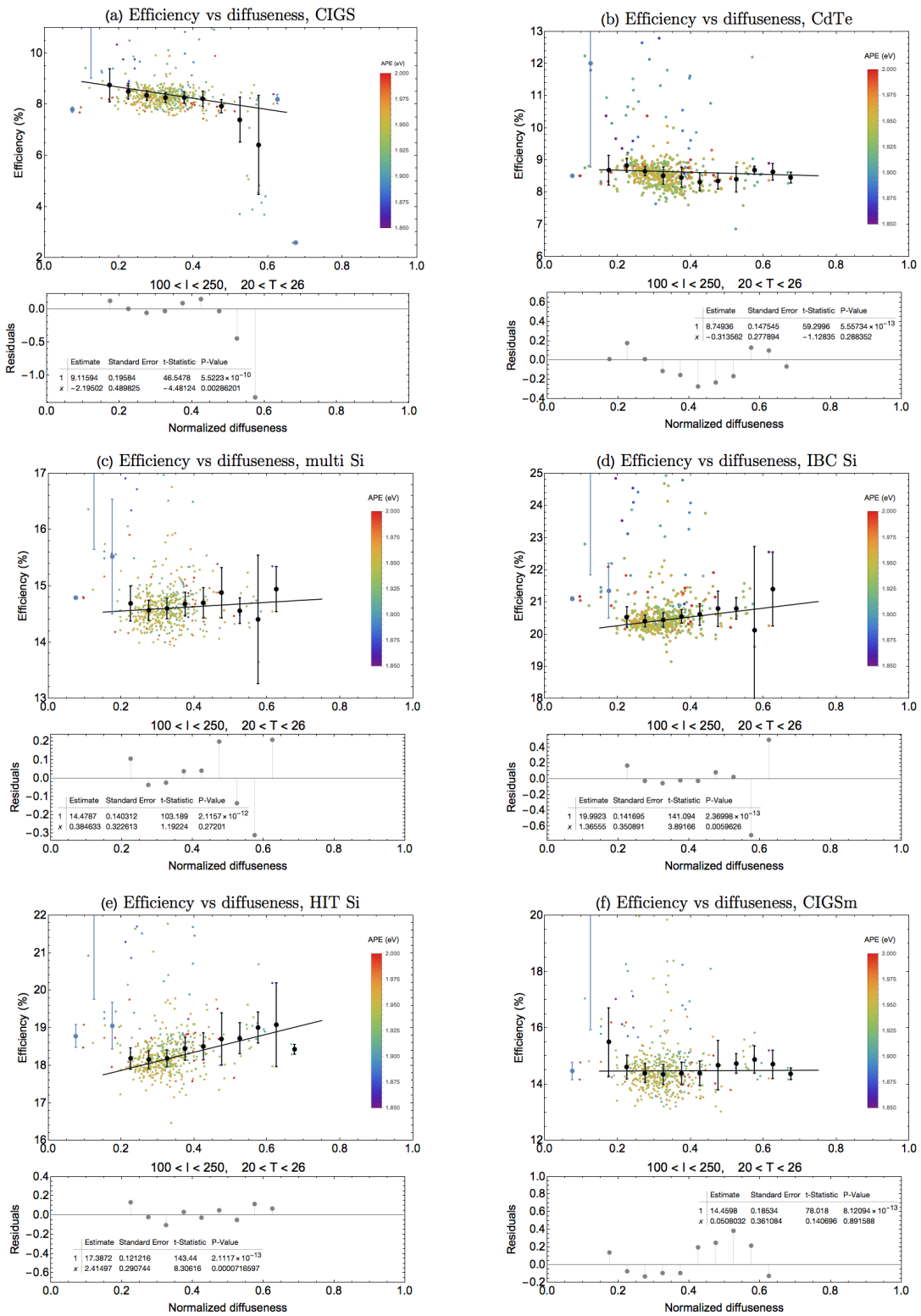


FIGURE 4.7: Efficiency against diffuseness for the six different modules. Small dots represent separate data points and are colored according to the APE. Black and blue dots represent the median efficiency over a range of 0.05 of diffuseness, while the blue dots have not been used for the fit as they represented too little data or unrealistic values of efficiency. The black line is a linear fit of the data and below the graphs are the residuals as well as the statistical parameters.

In Appendix B two sets of six graphs are added, here in the first set we have selected for irradiance and in the second for temperature. As the selections are separate, more data points remain. In these graphs, the same tendencies arose, with a clear negative relation for the flexible CIGS module, no clear relations for the CdTe and the CIGSm modules and significant relations for two of the three silicon cells. We have verified that for some other ranges of temperature and irradiance the same trends remain, however, further research could investigate whether the same conclusion holds for a larger variety of selections of temperature and irradiance.

This analysis shows that for the investigated solar cells, diffuseness is not likely to be an explanation for a higher performance ratio of thin film solar cells. In fact, the silicon cells are positively impacted by diffuseness, as opposed to the thin film cells which are either negatively impacted or not impacted by diffuseness. More likely causes of a higher performance ratio are therefore better efficiencies at lower irradiance, lower temperature coefficients and a broader spectrum sensitivity.

Further research could be done in order to investigate which other factors mainly lead to a high PR of thin film cells. A preliminary example of such an analysis is shown in Appendix C, here the influence of temperature is quantified, with small ranges selected for APE and irradiance.

More research will need to be done in order to investigate whether the same conclusion holds, when measuring over a longer period of time. This research has also shown that there can be great differences between several types of thin film solar cells, even when based on the same material. It is therefore relevant to further research the impact of diffuseness on a wider range of solar cell types and materials.

## Chapter 5

# Conclusions

Many of the thin film solar cells are claimed to have a higher performance ratio than silicon cells. In order to investigate whether diffuseness partially explains this higher PR, we measure the efficiency and module temperature of six types of commercially available solar panels, while also measuring the APE, irradiance and diffuseness. The diffuseness is measured using a cubic illuminance meter. Our results show that the cubic illuminance meter could potentially be a valid and affordable alternative for a sun tracker. It correlates reasonably well with the data of a sun tracker, with an  $R^2$  of 0.57 and a p-value of  $3.25 * 10^{-26}$  for the slope of the fit. It has the added benefit of not being able to erroneously exceed 1.

In order to verify the premise that some of the thin film solar cells have a higher performance ratio than silicon cells, we calculate the PR of all six modules. We find that the CIGSm has the highest PR of 101% in June/May and 95.5% over a year, while the silicon cells all had a PR of around 90%. The CdTe and flexible CIGS cells had a remarkably low PR at around 60%. This means that not all thin film solar cells have a higher PR, and that our research mainly focuses on the CIGSm module as it has the higher PR we are investigating.

The measurements of the cubic illuminance meter, when compared to irradiance and module temperature, show a clear correlation, here diffuseness decreases with  $0.123 \pm 0.012$  per  $1000 \text{ W/m}^2$ , and diffuseness decreases;  $0.0021 \pm 0.00021$  per  $^{\circ}\text{C}$ . These correlations are expected, and hence further suggest that the cubic illuminance meter measures a sensible definition of diffuseness.

Furthermore, we find that diffuseness clearly correlates with the efficiency of the six solar panels, here diffuseness increased the efficiency except for the flexible CIGS module, where diffuseness decreased the efficiency. In order to find out whether diffuseness was

actually causing this correlation, we analyzed the same correlations while selecting a small range of temperature and irradiance. This showed that diffuseness has a negative impact on the flexible CIGS module with a slope of  $-3.98 \pm 0.4$  efficiency percentage point per normalized diffuseness metric. Diffuseness has a positive effect on two of the silicon cells;  $2.72 \pm 0.86$  for the HIT Si cell and  $1.94 \pm 1.35$  for the IBC Si cell. While on the CdTe and CIGSm cell the impact was not significant.

From these analyses, we conclude that diffuseness is not a likely cause for a higher performance ratio of thin film solar cells. In fact, when holding other variables constant, we measured the silicon cells to perform better under diffuse light than thin film cells. This means that when thin film solar cells have a higher performance ratio, it is likely caused by other factors than light diffuseness. Possible factors are better performance under low intensities, under higher temperatures or lower spectra.

However, more research needs to be done in order to test this conclusion. We have measured the diffuseness for 33 days. It would therefore be relevant to carry out the research over a longer measurement period to investigate whether the same conclusion holds. Especially, because we are using a method where large amounts of data are necessary a longer period of measurement would further strengthen the research. It could also investigate whether some significant relations can be found between diffuseness and the flexible CIGS and CdTe modules, when looking over a longer period of time.

In this research we have verified for some other ranges of temperature and irradiance that similar patterns were visible, however further research could verify whether this is the case for all ranges of temperature and irradiance. Furthermore, we have found that there can be significant differences between similar solar cell types, which makes it relevant to carry out a similar research on a larger amount of solar cell types, to be able to map the characteristics of a large variety of thin film solar cells.

In order to further clarify the effect of diffuseness, it would be useful to carry out experiments in a lab situation, by aiming to exclusively change diffuseness while holding all other quantities constant. The lab research on the effects of diffuseness that has been done is still preliminary and measured only for two discrete values of diffuseness (Mohanty and Wittkopf, 2016).

Also, more research needs to be done on the cubic illuminance meter. Especially a longer measurement period to compare the sun tracker and cubic illuminance meter could further clarify the relation between the two ways of measuring diffuseness, and further verify the validity of the cubic illuminance meter as a sensor for diffuseness in the realm of solar cell science. The cube quantifies diffuseness based on the light from all directions, whereas monofacial solar cells are only impacted by the light from half of

---

all directions. Hence, a new design for the cube, specifically equipped for measurements on monofacial solar cells, could be a hemisphere with a number of light sensors, which only measure in half of all directions. For this, a new mathematical definition would need to be formulated, but it could further perfect the affordable alternative of a sun tracker.

## Appendix A

### 3D drawings of both cubes

In this appendix, we have added two 3D drawings of the first and second cube, in order to clarify the design of the cubes. The drawings only show the basis of the cubes, on top of all sides the sensors are placed and inside the cube are the sub-modules of the sensors. Around the first cube an extra perspex cube was placed for weather proofness. On the second cube watch glasses were placed over the sensors.

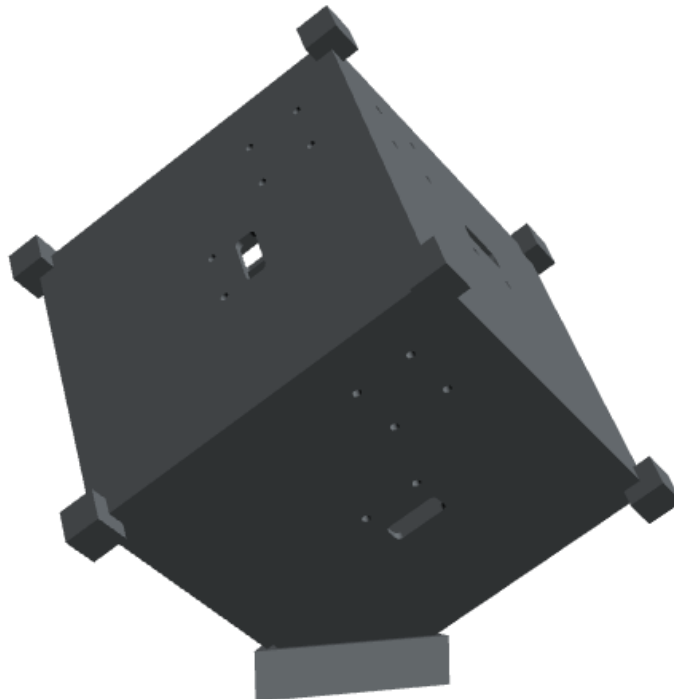


FIGURE A.1: 3D drawing of first cube

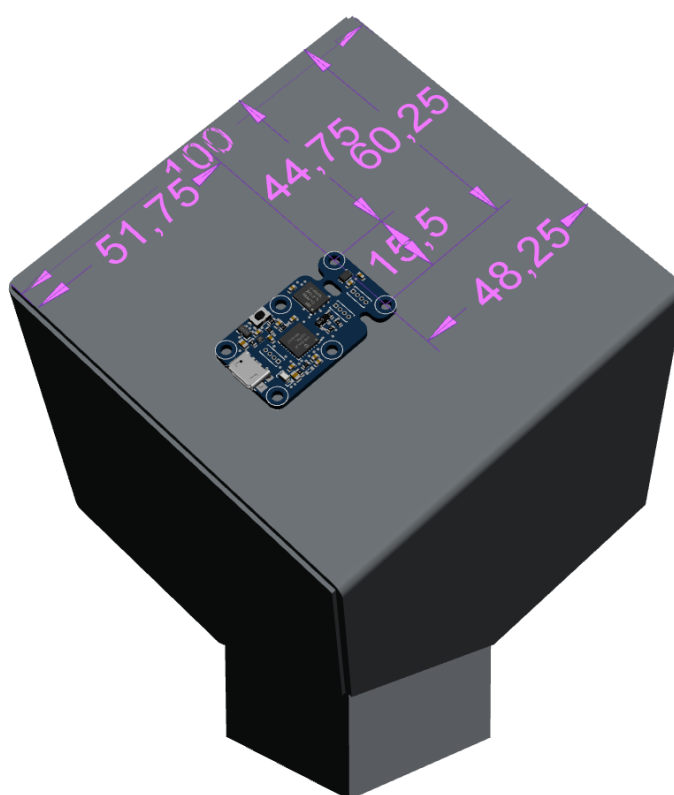


FIGURE A.2: 3D drawing of second cube

## Appendix B

# Additional graphs; efficiency against diffuseness binned separately

In the following appendix, we have added two sets of six graphs that serve to further justify our conclusion. In these graphs, we have used slightly different ranges of temperature or irradiance. Also, the temperature and irradiance have been selected separately. Despite the different binning, the same trends arise.

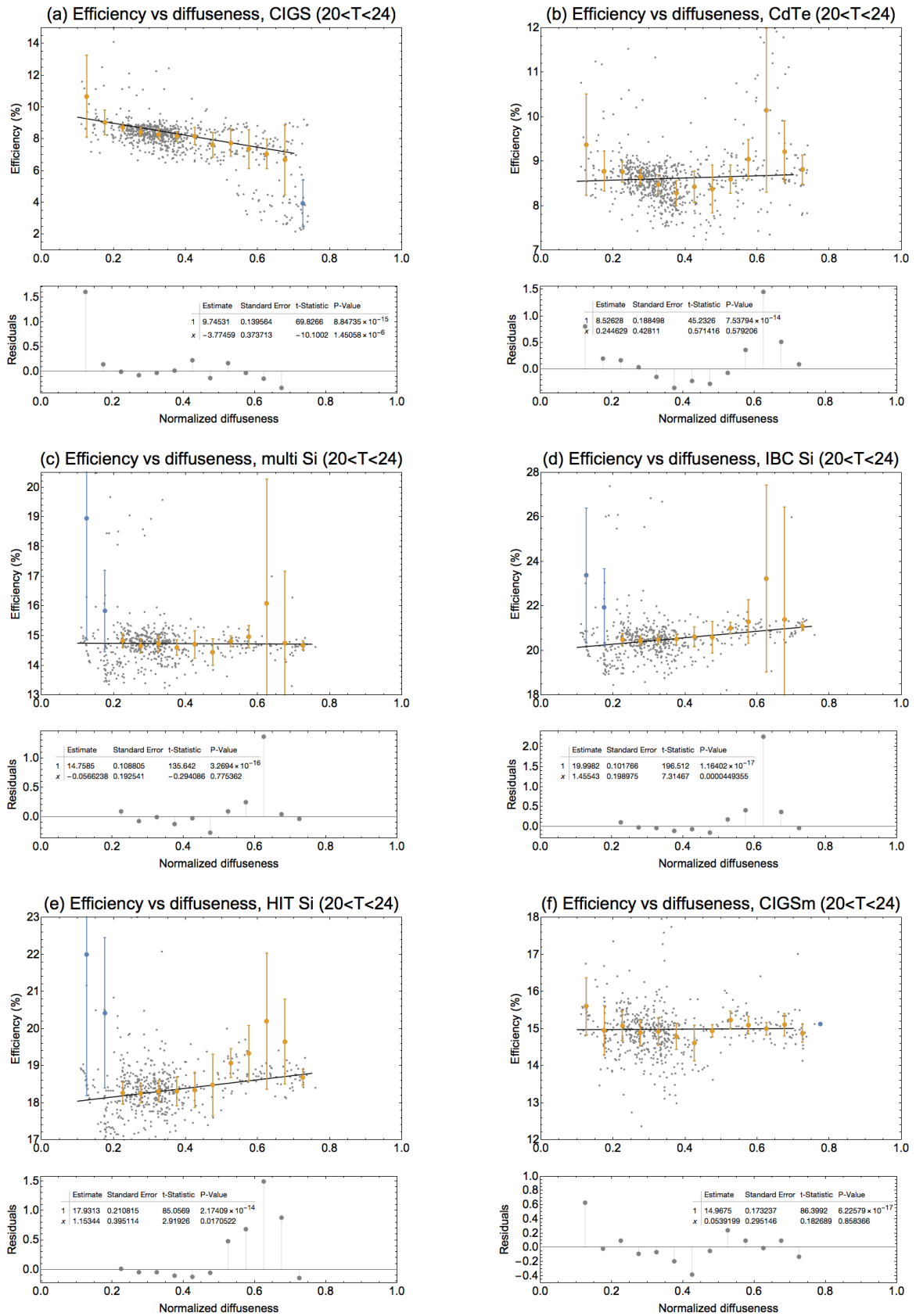


FIGURE B.1: Efficiency of all six modules vs diffuseness. Gray dots represent single data points, yellow and blue dots are the median efficiency over a range of 0.05 of diffuseness, blue dots were not used for the fit as they represented too little data or unrealistic values of efficiency. For these graphs a selection has been made for irradiance to be between 20 and 24  $C$

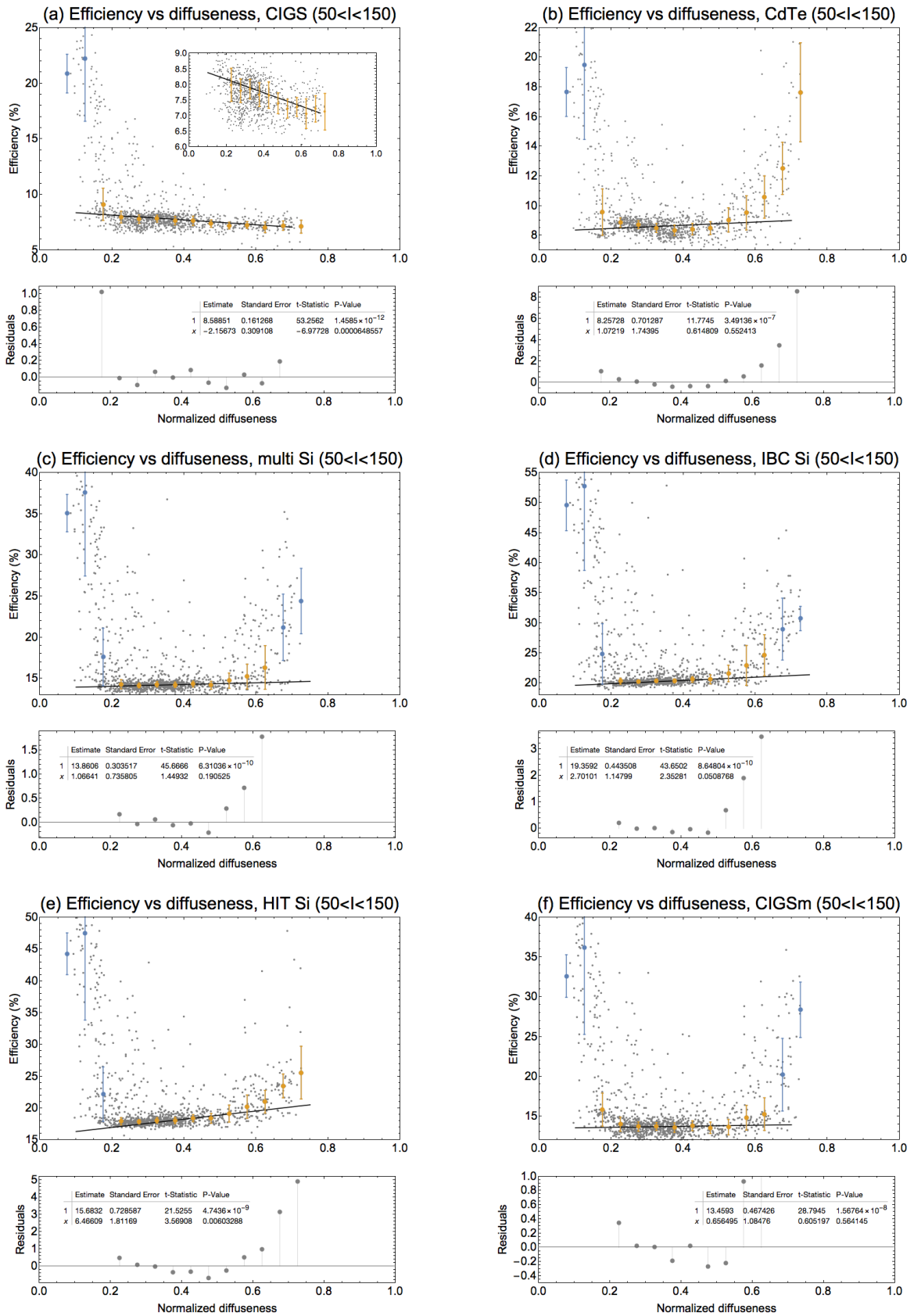


FIGURE B.2: Efficiency of all six modules vs diffuseness. Gray dots represent single data points, yellow and blue dots are the median efficiency over a range of 0.05 of diffuseness, blue dots were not used for the fit as they represented too little data or unrealistic values of efficiency. For these graphs a selection has been made for irradiance to be between 50 and 150 W/m<sup>2</sup>.

## Appendix C

# Additional graphs; efficiency against temperature

In this Appendix an example is given on how further research could be executed to analyze which other factors cause a higher PR of thin film solar cells. In these six graphs the temperature dependence is graphed, with a small range selected for irradiance and APE and the dots are colored for diffuseness.

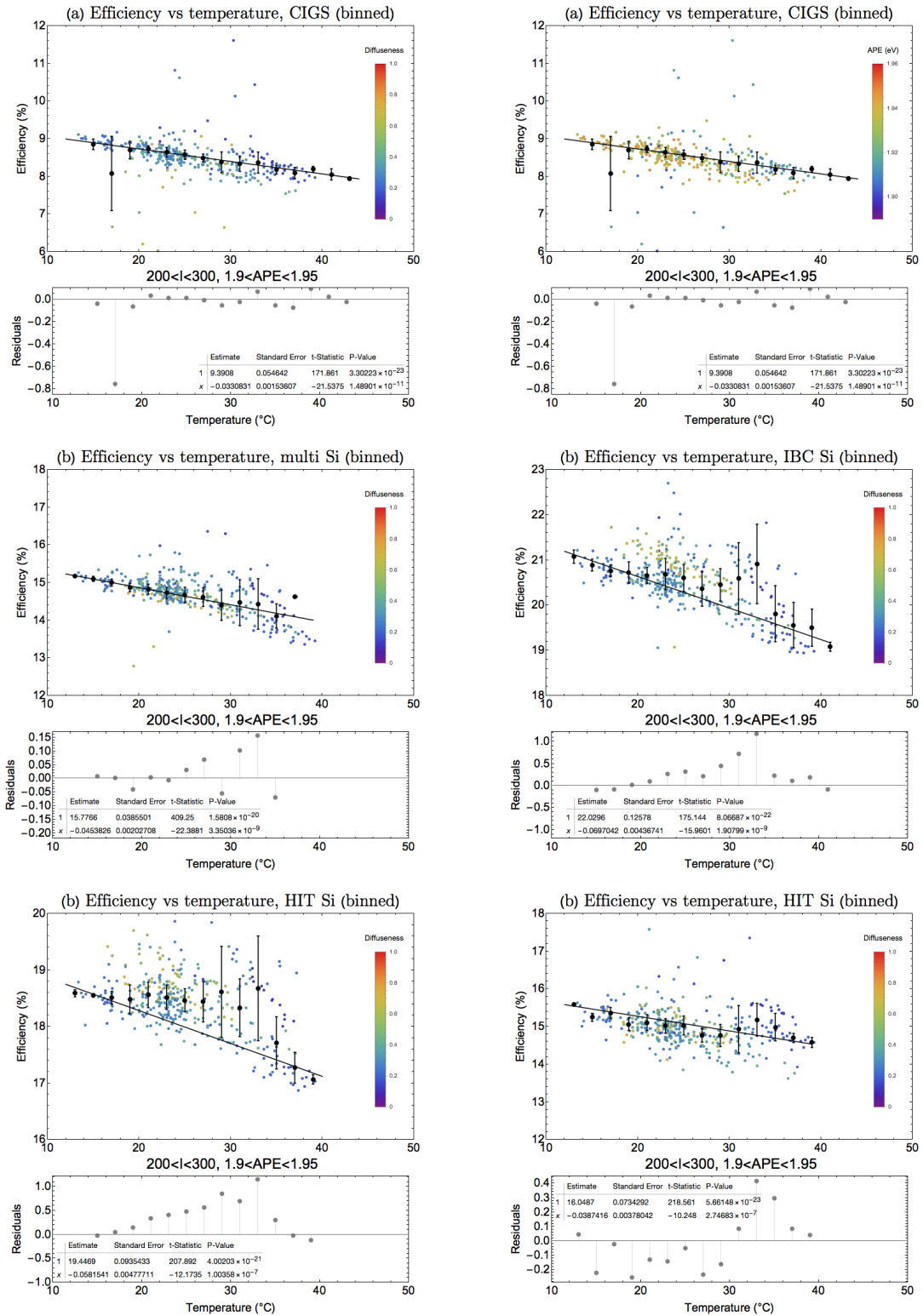


FIGURE C.1: Efficiency of all six modules against temperature, with the irradiance between 200 and 300  $\text{W}/\text{m}^2$  and the APE between 1.9 and 1.95 eV. The small dots represent single data points, the colors of these dots represent the diffuseness, the black dots are the median efficiency over a range of  $2^\circ$  of temperature. The error bars show the median deviation. The black line represents a linear fit of the data. Below the graph are the residuals of the fit as well as the statistical parameters.

# Bibliography

Burns, W. C. (1997). Spurious correlations.

Retrieved from <http://www.burns.com/wcbspurcorl.htm>.

Christian (2013). The width of the space charge region in a pn-junction. Retrieved from: <https://physics.stackexchange.com/questions/243172/the-width-of-the-space-charge-region-in-a-pn-junction>.

Cuttle, C. (1967). Beyond the working plane. In *Proceeding of the CIE Conference, 1967. 6*.

Cuttle, C. (2014). Research note: A practical approach to cubic illuminance measurement. *Lighting Research & Technology*, 46(1):31–34. test.

Fathi, M., Abderrezek, M., Djahli, F., and Ayad, M. (2015). Study of thin film solar cells in high temperature condition. *Energy Procedia*, 74:1410–1417.

Futscher, M. H. and Ehrler, B. (2016). Efficiency limit of perovskite/si tandem solar cells. *ACS Energy Letters*, 1(4):863–868.

Global Solar (2017). Cigs flexible solar panels. Retrieved from <http://www.globalsolar.com/>.

Green, M. A., Hishikawa, Y., Warta, W., Dunlop, E. D., Levi, D. H., Hohl-Ebinger, J., and Ho-Baillie, A. W. (2017). Solar cell efficiency tables (version 50). *Progress in Photovoltaics: Research and Applications*, 25(7):668–676.

Heliatek (2017). Heliacell, unique product properties. Retrieved from <http://www.heliatek.com/en/heliacell/unique>.

Janssen, G. J., Van Aken, B. B., Carr, A. J., and Mewe, A. A. (2015). Outdoor performance of bifacial modules by measurements and modelling. *Energy Procedia*, 77:364–373.

Kosten, E. D., Atwater, J. H., Parsons, J., Polman, A., and Atwater, H. A. (2013). Highly efficient gaas solar cells by limiting light emission angle. *Light: Science & Applications*, 2(1):e45.

- Mahato, N., Ansari, M. O., and Cho, M. H. (2015). Production of utilizable energy from renewable resources: Mechanism, machinery and effect on environment. In *Advanced Materials Research*, volume 1116, pages 1–32. Trans Tech Publ.
- Marion, B., Adelstein, J., Boyle, K., Hayden, H., Hammond, B., Fletcher, T., Canada, B., Narang, D., Kimber, A., Mitchell, L., et al. (2005). Performance parameters for grid-connected pv systems. In *Photovoltaic Specialists Conference, 2005. Conference Record of the Thirty-first IEEE*, pages 1601–1606. IEEE.
- Mohanty, L. and Wittkopf, S. K. (2016). Effect of diffusion of light on thin-film photovoltaic laminates. *Results in Physics*, 6:61–66.
- Nelson, J. (2003). *The physics of solar cells*. World Scientific Publishing Co Inc.
- O’regan, B. and Grätzel, M. (1991). A low-cost, high-efficiency solar cell based on dye-sensitized. *nature*, 353(6346):737–740.
- Polman, A., Knight, M., Garnett, E. C., Ehrler, B., and Sinke, W. C. (2016). Photovoltaic materials: Present efficiencies and future challenges. *Science*, 352(6283):aad4424.
- Rohde, R. A. (2007). Global warming art project. Retrieved from [https://www.researchgate.net/figure/221929763\\_fig2.Fig-2-Spectrum-of-solar-radiation-above-the-atmosphere-and-sea-level-prepared-by](https://www.researchgate.net/figure/221929763_fig2.Fig-2-Spectrum-of-solar-radiation-above-the-atmosphere-and-sea-level-prepared-by).
- Schweiger, M., Ulrich, M., Nixdorf, I., Rimmelspacher, L., Jahn, U., and Herrmann, W. (2012). Spectral analysis of various thin-film modules using high-precision spectral response data and solar spectral irradiance data. In *27th European Photovoltaic Solar Energy Conference and Exhibition, Frankfurt, Germany*, pages 3284–3290.
- Smets, A. H., Jäger, K., Isabella, O., van Swaaij, R. A., and Zeman, M. (2016). *Solar Energy: The physics and engineering of photovoltaic conversion, technologies and systems*. UIT Cambridge Limited.
- Wei, J. (2015). Measuring the i-v characteristic of pn junction devices with hf2li lock-in amplifier.
- White Paper Initiative (2015). White paper for cigs thin film solar cell technology. Retrieved from <http://cigs-pv.net/wortpresse/wp-content/uploads/2015/12/CIGS-WhitePaper.pdf>.
- Xia, L., Pont, S., and Heynderickx, I. (2016). Light diffuseness metric, part 2: Describing, measuring and visualising the light flow and diffuseness in three-dimensional spaces. *Lighting Research & Technology*, page 1477153516631392.

- Xia, L., Pont, S., and Heynderickx, I. (2017). Light diffuseness metric part 1: Theory. *Lighting Research & Technology*, 49(4):411–427.